AN ABSTRACT OF THE THESIS OF

Stephanie L. Ness for the degree of Master of Science in Chemistry presented on September 16, 1999. Title: Evidence for a Stepwise Mechanism in the Cycloreversion of Rhenium Diolates.

Redacted for Privacy

Abstract Approved: _____
Kevin P. Gable

The isotopically labeled diol, 1-^{18}O-*trans*-cyclooctane-1,2-diol, was synthesized by acid catalyzed ring-opening of the Z-cyclooctene in the presence of $H_2{}^{18}O$. A rhenium diolate, tris-(3,5-dimethylpyrazolyl)-hydridoboratorhenium (V) (oxo)*trans*-1,2-cyclooctanediolate, was synthesized and heated at 110°C for 17 hours, and shown to be thermodynamically stable. The isotopically labeled diol was then used to incorporate ^{18}O into the diolate positions of tris-(3,5-dimethylpyrazolyl)-hydridoboratorhenium (V) (oxo)(*trans*-1,2-cyclooctanediolate). The level of ^{18}O incorporation in the diol was measured by ^{13}C NMR, and the level of ^{18}O incorporation in the rhenium diolate complex was measured by mass spectroscopy and found to be 19.2 ± 2.2 %. The labeled diolate complex was heated at 106°C in sealed NMR tubes for different periods of time. After heating the diolate, more oxygen-18 had moved out of one position than the other, as measured by relative peak heights (shifted peak/normal peak). These experiments support the hypothesis that the cycloreversion of rhenium diolates is a stepwise process.

Evidence for a Stepwise Mechanism in the Cycloreversion of Rhenium Diolates

by

Stephanie L. Ness

A THESIS

submitted to

Oregon State University

in partial fulfillment of
the requirements for the
degree of

Master of Science

Presented September 16, 1999
Commencement June 2000

Master of Science thesis of Stephanie L. Ness presented on September 16, 1999

APPROVED:

Redacted for Privacy

Major Professor, representing Chemistry

Redacted for Privacy

Chair of Department of Chemistry

Redacted for Privacy

Dean of Graduate School

I understand that my thesis will become part of the permanent collection of Oregon State University libraries. My signature below authorizes release of my thesis to any reader upon request.

Redacted for Privacy

Stephanie L. Ness, Author

ACKNOWLEDGMENTS

I am very grateful for the help of many people who made the writing of this thesis possible. I would first of all like to thank my advisor, Dr. Gable, who helped me every step of the way with the research as well as offering suggestions for this thesis. His help was invaluable and is greatly appreciated. I would also like to thank Rodger Kohnert for his helpful advice concerning the NMR experiments. I am indebted to Dr. Alex Yokochi for obtaining the x-ray crystal structure of tetrachloro-μ-oxodioxotetrakis-3,5-dimethylpyrazoledirhenium (V). I also received help from members of the Gable group, especially Dr. Abdullah AbuBaker, Eric Brown, and Fedor Zhuravlev, for which I am grateful. My family has also been extremely supportive; this is especially true of my Mother, Carol Ness.

TABLE OF CONTENTS

TABLE OF CONTENTS (Continued)

Page

TABLE OF CONTENTS (Continued)

Page

LIST OF FIGURES

LIST OF FIGURES (Continued)

LIST OF TABLES

LIST OF APPENDIX TABLES

Evidence for a Stepwise Mechanism in the Cycloreversion of Rhenium Diolates

Chapter 1. Introduction and Literature Review

General Examples of Hydrocarbon Oxidations

The oxidation of olefins using metal oxides is a very important process. There are three basic categories of metal-catalyzed olefin oxidations; these are epoxidation, C-H activation, and dihydroxylation. The first of these, epoxidation, is frequently followed by hydrolytic ring-opening of the epoxide to form a diol. This epoxidation can use molecular oxygen as the oxygen source with high yields in some cases. One example of this is the process used to make ethylene glycol, in which silver[1] is used as the catalyst (Figure 1.1). This type of oxidation can be made enantiospecific if the olefin

Figure 1.1: Silver Catalyzed Epoxidation

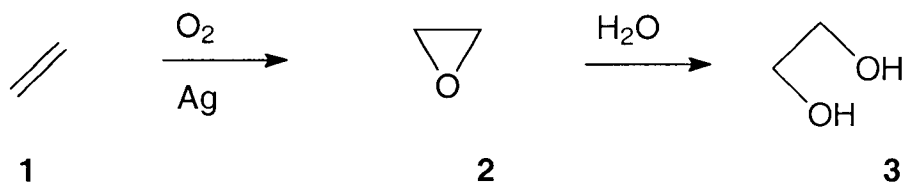

1 2 3

in question is an allylic alcohol. The Sharpless epoxidation[2] of allylic alcohols uses titanium(IV) alkoxides treated with tartrate esters as the catalyst (Figure 1.2). The Jacobsen reaction[3] is another example of this, only in this case high enantioselectivity

can be seen also for non-directing alkenes. A second process, C-H activation, is used in functionalization of alkanes. One example of this is the Shilov reaction,[4] which uses

Figure 1.2: Sharpless Epoxidation

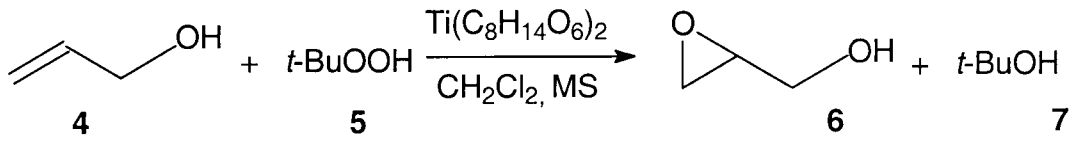

a mixture of platinum (II) tetrachloride and platinum(IV) hexachloride in the presence of water to transform methane into a mixture of methanol and methyl chloride. The Catalytica process[5] is similar, but the catalyst in this case is a mercury (II) salt (Figure 1.3). This reaction has the advantage of producing methanol without the methyl chloride by-product.

A third process, dihydroxylation of olefins, can be carried out with osmium tetraoxide or potassium permaganate. A disadvantage of the osmium tetraoxide dihydroxylation relative to the epoxidation reaction is that attempts to use molecular oxygen as the oxygen source are not successful–N-methylmorpholine-N-oxide (NMO) is used as the stoichiometric oxygen source[6](Figure 1.4). Nevertheless, this reaction is used in production of fine chemicals, which only comprise 3% of all chemicals made but account for 20% of industry profits.[7] Osmium tetraoxide catalyzed dihydroxylation is especially useful in the synthesis of cortisone[8] and other pharmaceuticals. An advantage of this reaction is that it can be made enantioselective. This is achieved by

addition of a chiral ligand[9] such as dihydroquinidine-4-chlorobenzoate. A better understanding of the mechanism of this reaction could allow for the development of other catalysts for this reaction. The expense of osmium by itself is sufficient to warrant such an investigation.

Figure 1.3: Catalytica Process

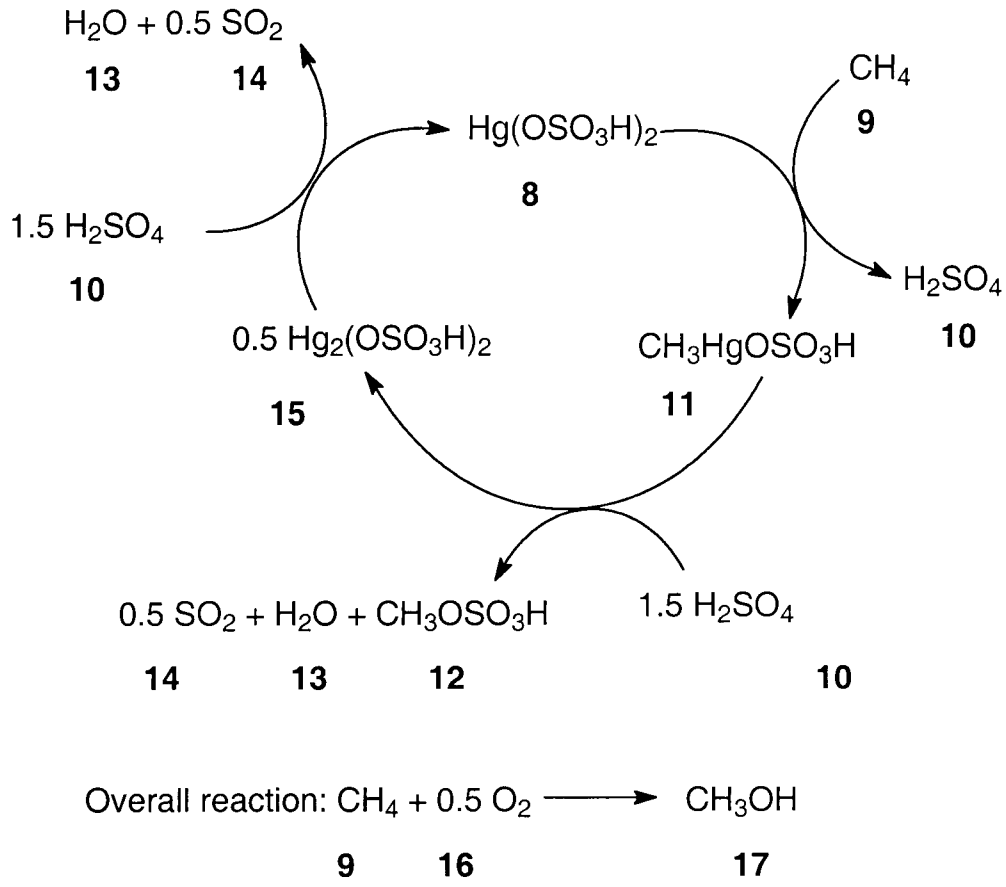

Figure 1.4: Dihydroxylation

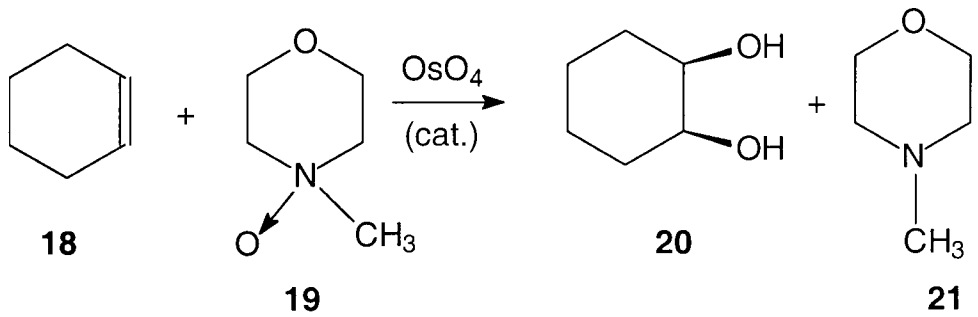

Basic Facts About the Dihydroxylation of Olefins

The basic mechanism of this reaction involves the formation of an intermediate with a five membered ring (see Figure 1.5). The reaction gives *syn* addition of hydroxyl groups across the double bond, much like the similar potassium permanganate oxidations of olefins. The kinetics of the reaction show that it is first order in olefin and first order in osmium tetraoxide, so both molecules must be involved in the rate determining step. Electron deficient alkenes react more slowly than electron rich alkenes, which leads to the assumption that the alkene functions as a nucleophile in the reaction. The rate is also greatly enhanced by the presence of amine ligands.[10] This is probably due to the fact that coordination of the amine with the osmium tetraoxide changes the electronic character of the complex. Exactly why this happens is not clear; addition of electron density from the amine ought to decrease the oxidizing ability of the metal. There are two possibilities–either the coordination of the amine changes the frontier orbitals, or the change from tetrahedral to trigonal bipyramidal geometry causes

Figure 1.5: Basic Mechanism of Dihydroxylation

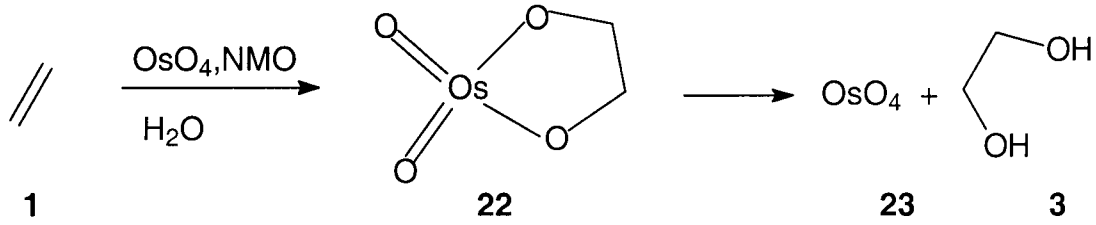

1 22 23 3

the increased reactivity. For the asymmetric reaction, when the dihydroquinidine (DHQD) ligand or the dihydroquinine (DHQ) ligand is used, the face selectivity is easily predicted and does not change with temperature.

The Stepwise vs. Concerted Mechanism Controversy

In recent years, there have been two major mechanisms proposed for this reaction. The first of these mechanisms, proposed by Criegee[11] and defended by Corey,[12] is shown in Figure 1.6. This is the classic concerted mechanism for this reaction. This mechanism is analogous to the mechanism for ozonolysis and other concerted organic cycloadditions. The *syn* addition across the double bond is consistent with this mechanism, as are the overall second-order kinetics. However, there are no other examples of this type of mechanism involving a transition metal.

The second mechanism, proposed by Sharpless,[13] is the stepwise mechanism involving the metallaoxetane intermediate shown in Figure 1.7. The original basis for this proposal was the fact, noted above, that electron rich alkenes react faster than electron poor alkenes. Since the osmium tetraoxide is seen as an electrophile, the idea

was that the more electrophilic metal center was likely to be involved in the formation of the transition state as well as the more electron rich oxygen. There is evidence that the formation of four membered rings from alkenes is common in transition metal chemistry. For example, the reaction of square planar complex $((CF_3)_2MeCO)_2(NAr)(CHtBu)W$ with trimethylsilylethene produces the tungsten

Figure 1.6: Concerted Mechanism

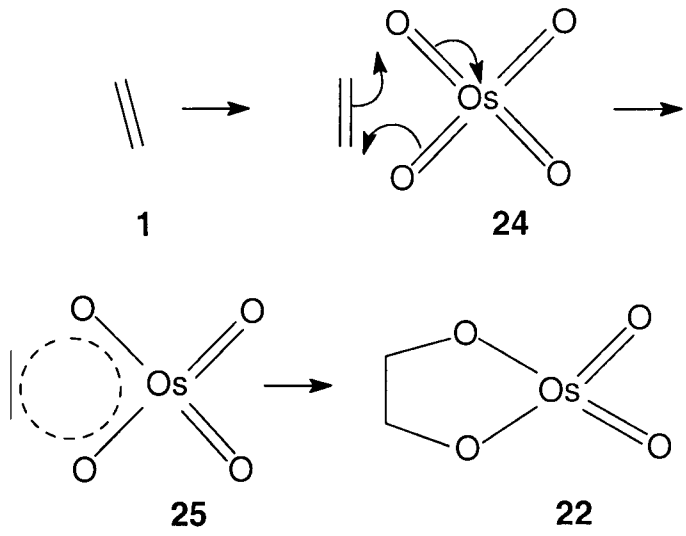

complex in Figure 1.8.[14] At the time that the concerted mechanism was proposed, there were no known examples of an alkyl group shifting[15] to an oxo ligand. However, there is now precedent for similar shifts to oxo groups from other transition metals.[15] One example[16] of this is shown in Figure 1.9.

Figure 1.7: Stepwise Mechanism

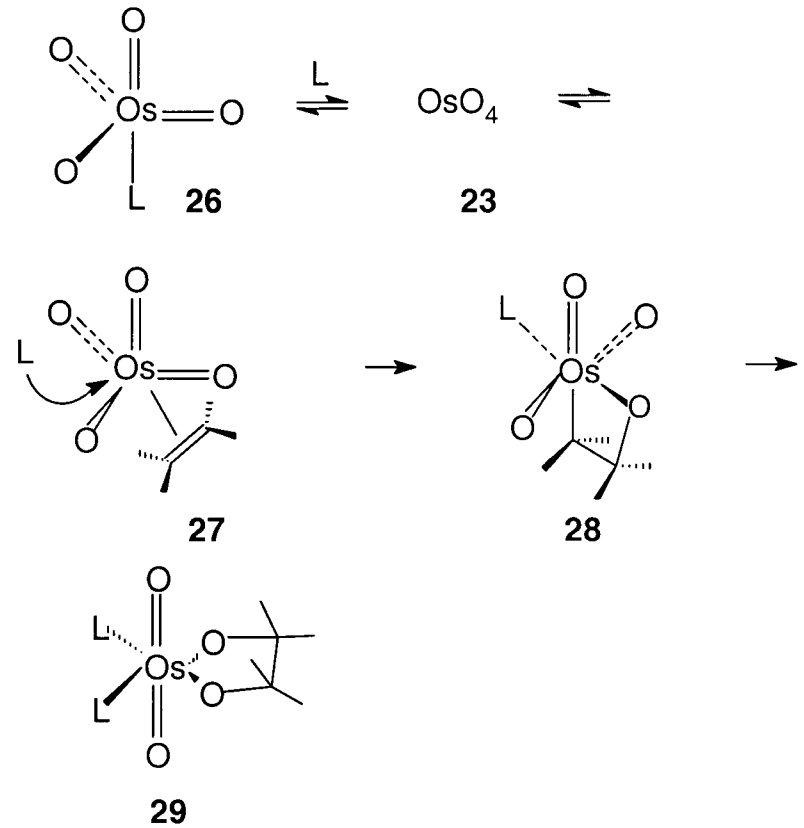

Induced Enantioselectivity as Evidence for the Stepwise Mechanism

This mechanism has the further advantage of explaining why the addition of chiral amine (**34**) in Figure 1.10 would cause this oxidation to be enantioselective. The rationale for this effect is that the bulky ligand and one carbon of the metallacycle are both directly attached to the metal. The asymmetric induction effect is much greater than would be expected for the concerted pathway, in which both carbons are removed from the metal center by one oxygen atom. Approach of the alkene might be expected to occur with as little interaction with the ligand as possible for steric reasons. However,

Figure 1.8: Formation of Four-Membered Ring

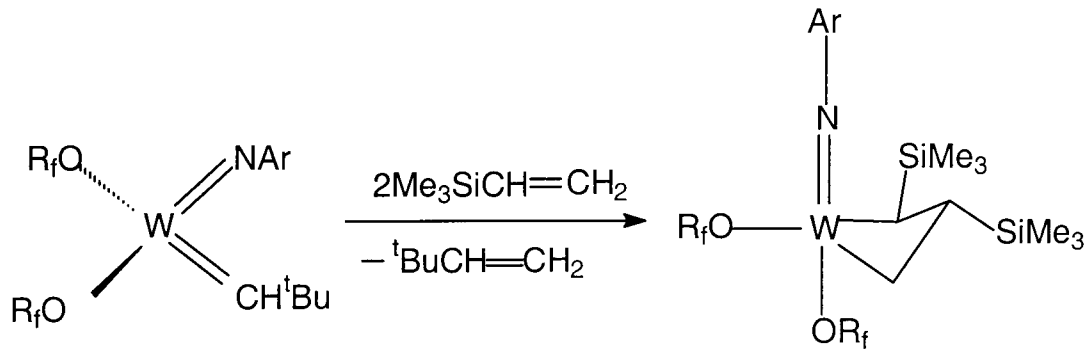

R_f = $CMe(CF_3)_2$

30 **31**

Figure 1.9: Example of Aryl to Oxo Shift

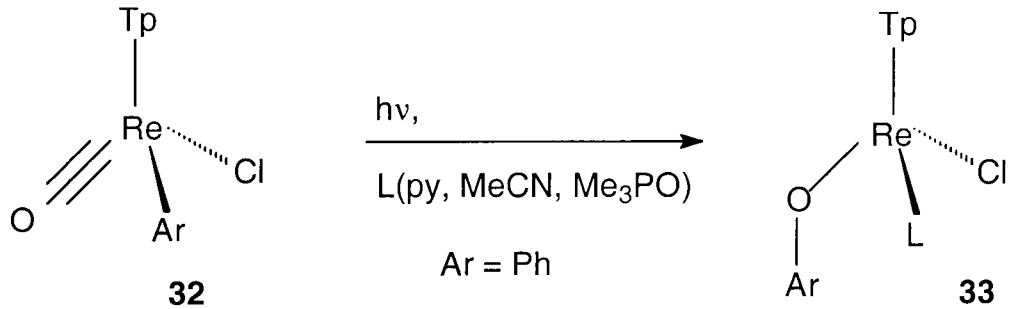

32 **33**

Figure 1.10: Amine Ligand (**34**)

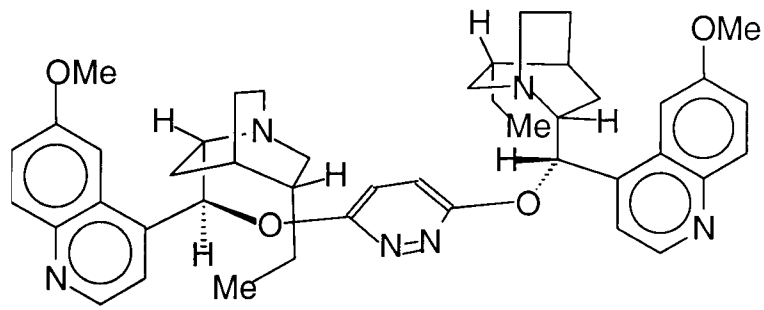

34

Corey has argued[17] that the stereoselectivity can be accounted for in a concerted mechanism if one takes formation of the intermediate (**35**) in Figure 1.11 to be the step prior to addition of olefin to the complex. The crystal structure of this compound only showed the two osmium clusters attached by the bridging ligand, not bridging oxos. (It also showed two free osmium tetraoxide molecules per unit cell.) The structure shown in Figure 1.11 was proposed because of differences in reactivity. First, Corey claimed that the hydroxylation of styrene is 100 times faster in the presence of the ligand in Figure 1.10, which is capable of linking two osmium centers together, than in the presence of the ligand in Figure 1.12, which cannot bring two osmium centers together. Another kinetic study used ^{19}F NMR to monitor the reaction of *o*-(triflouromethyl)styrene with a mixture of osmium tetraoxide and the bridging amine ligand in Figure 1.10. After one equivalent of the triflouromethylstyrene had reacted, a second equivalent was added. The reaction rate of the first equivalent was 20 times

faster than the rate of reaction for the second equivalent. From this kinetic data, Corey proposed the formation of the apparently short-lived bridged species in Figure 1.11.

Figure 1.11: Proposed Intermediate

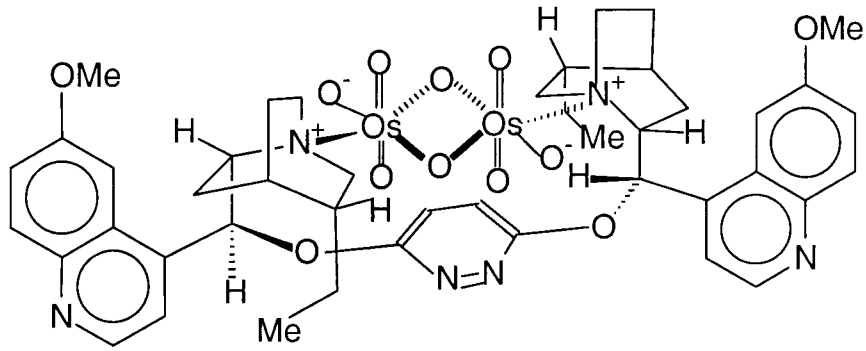

35

Computational Studies of the Two Mechanisms That Favor the [3+2] Mechanism

Computational chemistry has also been used to study the mechanisms. In 1997, a study was published using density functional theory which seemed to show that the metallaoxetane is too stable to be an intermediate.[18] The 5s, 5p, 5d, 6s, and 6p orbitals

Figure 1.12: Amine Ligand (**36**)

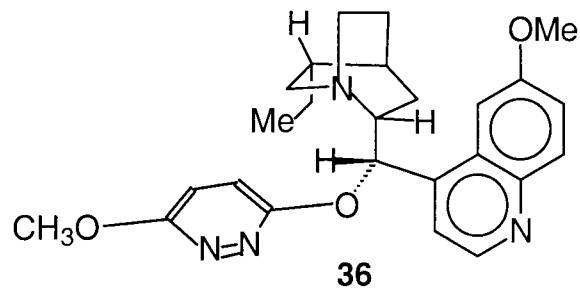

36

of osmium were approximated by an uncontracted triple-ζ STO basis set, and double ζ basis sets were used for carbon, oxygen, nitrogen, and hydrogen. Torrent, et. al. found[18] that the metallaoxetane is 3.7 kcal/mol above the reactants. The energy of the calculated transition state (TS) required to form this metallaoxetane is calculated at 39.7 kcal/mol higher than the energy of the reactants, and therefore the metallaoxetane would not form under the mild conditions typical of the dihydroxylation reaction. So, if the metallaoxetane formed, the energy barrier would prohibit equilibration between it and the reacting olefin and osmium tetraoxide. It would therefore be quite stable if it ever formed. The energies of the [2+3] transition states, on the other hand, were calculated at between 1.1 and 2 kcal/mol above the energy of the reactants, while the overall reaction was calculated to be exothermic. This led Torrent to support the concerted mechanism. One small difficulty that the authors had with the concerted mechanism is that they were unable to model the preliminary olefin coordination to osmium that is expected for the concerted mechanism. Another possible problem with this study is the lack of direct comparison of calculated vs. experimental values for their method.

Computational and Isotope Effects Study Supports a Concerted Mechanism

Another study that seems to favor the concerted mechanism compares experimental isotope effects with the calculated isotope effects for the concerted transition state and the stepwise metallaoxetane intermediate.[19] In this study, the amine ligand was modeled using ammonia, and the two alkenes used were propene and ethylene. The transition state for both the concerted and stepwise mechanisms for the reaction of osmium

tetraoxide with each olefin was found using Becke3LYP calculations with an effective core potential basis set for osmium with a (341/321/21) basis set for the "valence" electrons in conjunction with a 6-31G* basis set for all other atoms. The authors report that this shows the activation barriers for the concerted transition state range from 3.1-3.4 kcal/mol, while the activation barriers for the stepwise process are calculated to be between 41 and 44 kcal/mol. These energy values would suggest that the concerted mechanism is more reasonable. In addition, the ^{13}C isotope effects were also calculated for the two transition states, and these isotope effects were much more similar to experimental values. For example, the calculated values of the isotope effect for the reaction with propene are 0.907 and 0.909 at C-2. (These two values are calculated for two different concerted transition states.) The experimental values for the analogous isotope effect for *tert*-butylethylene are 0.906(9) (for a reaction carried to 90.5% completion) and 0.908(4) (for a reaction carried to 85.6% completion). In contrast, the calculated isotope effects for the formation of a metallaoxetane are 0.892 and 0.885. As noted above, the compound used in the experiments contains a *t*-butyl group where the two compounds used in the calculations contain a hydrogen or methyl group. The reason the *tert*-butylethylene was used for the experiment is that the bulky group prevents competing formation of mixtures of regioisomeric [2+2] pathway transition states. If mixtures of transition states formed, then the average isotope effect for all of them would be reflected in the experimental isotope effect, and the result would not be comparable to the calculated number.

Computational Studies That Favor the [2+2] Mechanism

However, there are conflicting computational studies showing that the stepwise mechanism is viable.[20] The Frenking study (ref. 20a) was an *ab initio* study using ECP basis set for osmium and an all electron basis set for all other atoms. The models made were of the osmium tetraoxide with coordinated ammonia, the metallaoxetane intermediate, the bridged structure proposed by Corey to be the reactive species, and a similar bridged structure containing the five-membered result of reaction with olefin. The ammonia was used to model the complex ligand in Figure 1.10. The bond lengths and angles of known species compared well to experimental values. One conclusion that was made was that the bridged species proposed by Corey would form more easily after the olefin reacted with the osmium; the energy of this bridged species was lower than the energy of the proposed initial bridged species. Corey's case depends on an initial bridged species before the reaction with olefin takes place, but this seems to indicate that if this does form, it would form after the reaction rather than before it. Frenking also found that the metallaoxetane is an energy minimum. A rather subtle argument for the stepwise mechanism from these results is the fact that the HOMO of the osmium complex is raised in energy when coordinated to ammonia, which would make nucleophilic attack on the olefin seem reasonable. However, electron withdrawing groups on the olefin, instead of easing the reaction as they should if there were nucleophilic attack, retard the reaction. The authors therefore rationalize that there are two steps--one nucleophilic attack and one electrophilic attack.

A second theoretical study by Sharpless and co-workers used density functional theory (ref. 20b). The group used ruthenium complexes to model the different kinds of metallaoxetanes, reactants, and products(see Figure 1.13). One weakness in this study is the lack of direct comparison with the experimental values. Since these ruthenium complexes are poorly characterized, the calculated bond lengths were compared to similar bond lengths in the analogous osmium complexes. The one direct comparison of experimental vs. calculated values is for ruthenium tetraoxide. This paper also suggests that the metallaoxetane has a reasonable energy--the highest energy metallaoxetane intermediate is 19 kJ/mol (4.5 kcal/mol) above the energy of the $RuO_3(NH_3)$ complex, while the lowest energy metallaoxetane intermediate is 10 kJ/mol (2.4 kcal/mol) above the energy of this complex.

Figure 1.13: Ruthenium Species

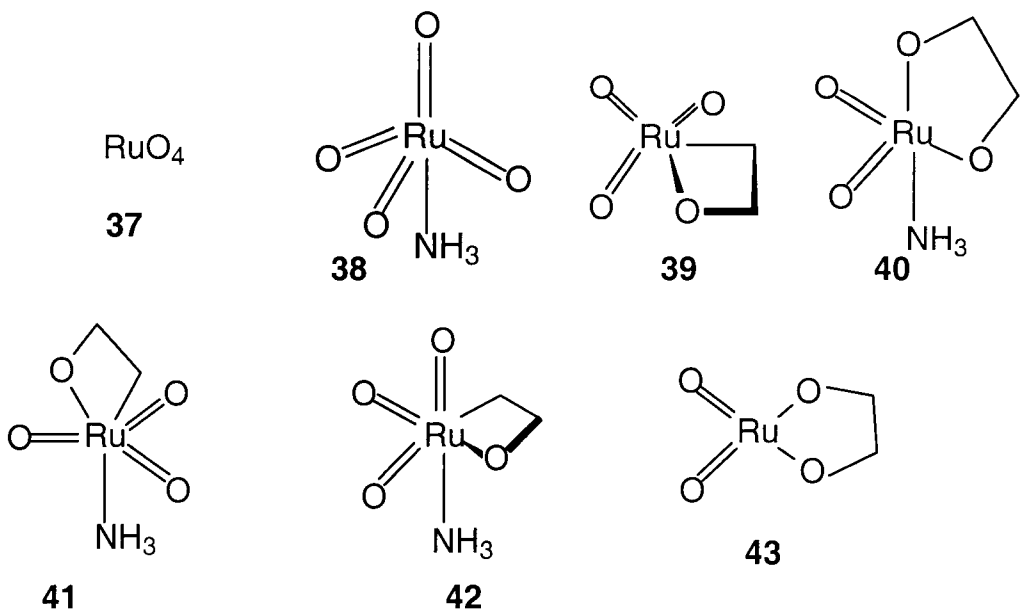

Eyring Plot Studies

A final argument in favor of the stepwise mechanism is a study of Eyring plots[21] for this reaction. The reaction that was studied is outlined in Figure 1.14. The modified Eyring equation used to study this reaction is derived below.

Equation1 $\ln (k/T) = C - (\Delta G^{\ddagger})/(RT)$,

where k= rate constant,

C = constant,

$\Delta G^{\ddagger}$ = Gibbs free energy of activation,

R = gas constant,

T = temperature in K

The relative rates for the two competing reactions can be expressed as:

$\ln (k_1/T) - \ln (k_2/T) = C - (\Delta G_1^{\ddagger})/(RT) - [C - (\Delta G_2^{\ddagger})/(RT)]$

$\ln k_1/k_2 = -(\Delta\Delta G^{\ddagger})/(RT)$

$\ln k_1/k_2 = -(\Delta\Delta H^{\ddagger} - T\Delta\Delta S^{\ddagger})/(RT)$

$\ln k_1/k_2 = -(\Delta\Delta H^{\ddagger})/(RT) + (\Delta\Delta S^{\ddagger})/(R)$

Figure 1.14: Dihydroxylation for Eyring Plot Studies

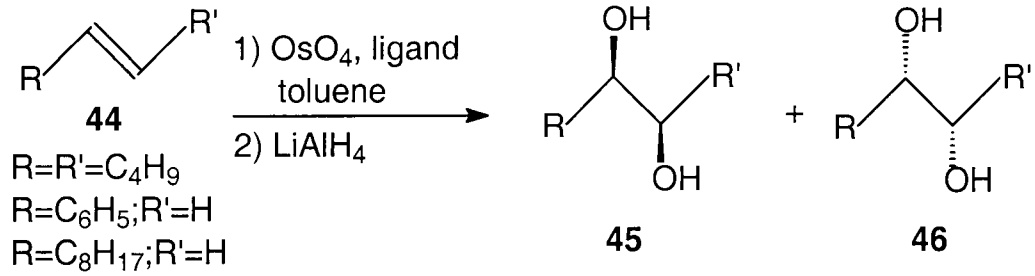

We can define a variable P as the ratio of rate constant for formation of major diol over that of minor diol in enantioselective generation of diol. For a series of alkenes the plots of ln P vs. 1/T for this reaction are all slightly bent.[21] This is consistent with a stepwise mechanism. If the process is concerted, the energy difference between diastereotopic transition states should lead to a linear modified Eyring plot, since there should only be one enthalpy of activation and entropy of activation. The changes in the slopes suggest that at least two processes are involved--either sequentially or in competition. The change in slope is usually caused by a change in rate determining step with temperature, which can only occur if there is more than one process. Unfortunately, however, it does not rule out the concerted mechanism. The bent lines of the Eyring plots are also consistent with competition between two different concerted transition states.

Use of Rhenium Diolates to Study the Dihydroxylation of Olefins

Gable and co-workers have done much work with rhenium diolates. These compounds are stable in the presence of air and only decompose slowly in solution at room temperature. The diolates can be isolated as pure compounds.[22] They were initially synthesized by reaction of an alkali diolate dissolved in that same diol with pentamethylcyclopentadienyl (Cp*) rhenium (oxo) dichloride.[23] This reaction required that the dichloride be made first and that the diol that was used be a liquid. A better method was devised in which the Cp^*ReO_3 was reduced with triphenylphosphine to the dioxide *in situ*, and the dioxide condensed with diol in the same reaction pot to produce

the diolate.[24] The above example used a diolate with the pentamethylcyclopentadienyl ligand, but the method works not just for cyclopentadienyl ligand analogs but also for the hydrido-*tris*-(pyrazolyl)borate (Tp) ligand and its analogs.[25]

The reaction that this group has studied is the cycloreversion of rhenium diolate complexes. Since this reaction is the microscopic reverse of the osmium tetraoxide oxidation, it is therefore possible to draw formal conclusions about the osmium tetraoxide oxidation by the principle of microscopic reversibility.[26] This process, shown in Figure 1.15, was demonstrated for pentamethylcyclopentadienyl rhenium (oxo) ethanediolate complex by Herrmann in 1987.[27] This process has also been shown to occur in diolates containing the hydrido-*tris*-(3,5-dimethylpyrazolyl) borate[28] (Tp') ligand. Several advantages of studying this cycloreversion instead of directly studying the osmium tetraoxide oxidation reaction exist. The diolates do not exhibit flexible coordination chemistry seen in osmium oxides;[29] therefore it is easier to determine effects of ligands on the system. The cycloreversions also proceed in nonpolar solvents and are slower than the osmium tetraoxide oxidation.[30]

Figure 1.15: Cycloreversion

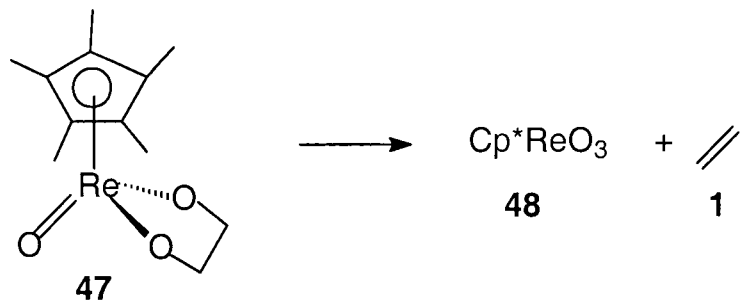

47 **48** **1**

Thermodynamic Study of Rhenium Diolates

Other work done by the Gable group shows that the cycloreversion is an entropically driven process.[31] As most rhenium diolate complexes undergo cycloreversion, the opposite occurrence with strained alkenes demonstrates the balance in thermodynamic driving force behind the reaction. The experiment that was done to show this involved sealing up Cp^*ReO_3 , norbornene, and benzene-d6 in an NMR tube and heating it to temperatures between 90 and 125 °C. The observed formation of two diolates in equilibrium with the reactants (see Figure 1.16) shows that the system is at a thermodynamic balance point. The equilibrium constant was also determined; at 122.4°C it is 11.4 ±1.5.

Study of Kinetics of Rhenium Diolates

In another study, Gable determined the rate constants, the enthalpy of activation, and the entropy of activation of alkene extrusion[32] from several diolates. The diolates used in these experiments are shown in Figure 1.17. The diolates were dissolved in benzene-d6 and sealed into NMR tubes under vacuum. The NMR tubes were then heated at different temperatures. The reaction progress was tracked by monitoring the ^1H NMR signals of the Cp* ligand. The reactions were first order and were followed for at least three half lives. The kinetics of the oxidation of norbornene by pentamethylcyclopentadienyl rhenium trioxide were also examined. For these experiments, an excess of about 5-10 equivalents of norbornene was used in order to

make the reaction pseudo-first-order. The observed rate constant was then determined. Since the equilibrium constants and the rate of approach to equilibrium were known at each temperature, the forward and reverse rate constants could be calculated using the following two equations: $K_{eq} = k_O / k_e$ and $k_{obs} = k_O[\text{norbornene}] + k_e$, where K_{eq} = equilibrium constant, k_O = rate of oxidation, and k_e = rate of alkene extrusion. The kinetics of oxidation of *trans*-cyclooctene and norbornadiene by Cp^*ReO_3 were examined in the same way. From the kinetic data, the enthalpy and entropy of activation were calculated. Some results of this study are shown in Table 1.1.

Figure 1.16: Cycloaddition / Cycloreversion

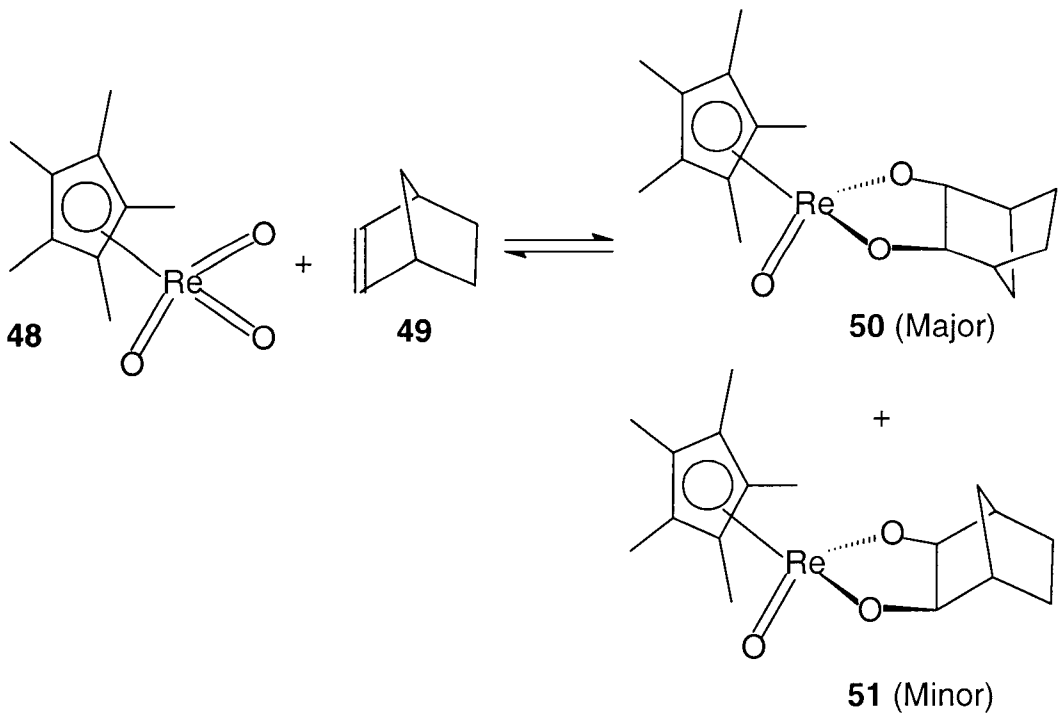

Figure 1.17: Diolates Used in Kinetics Experiments

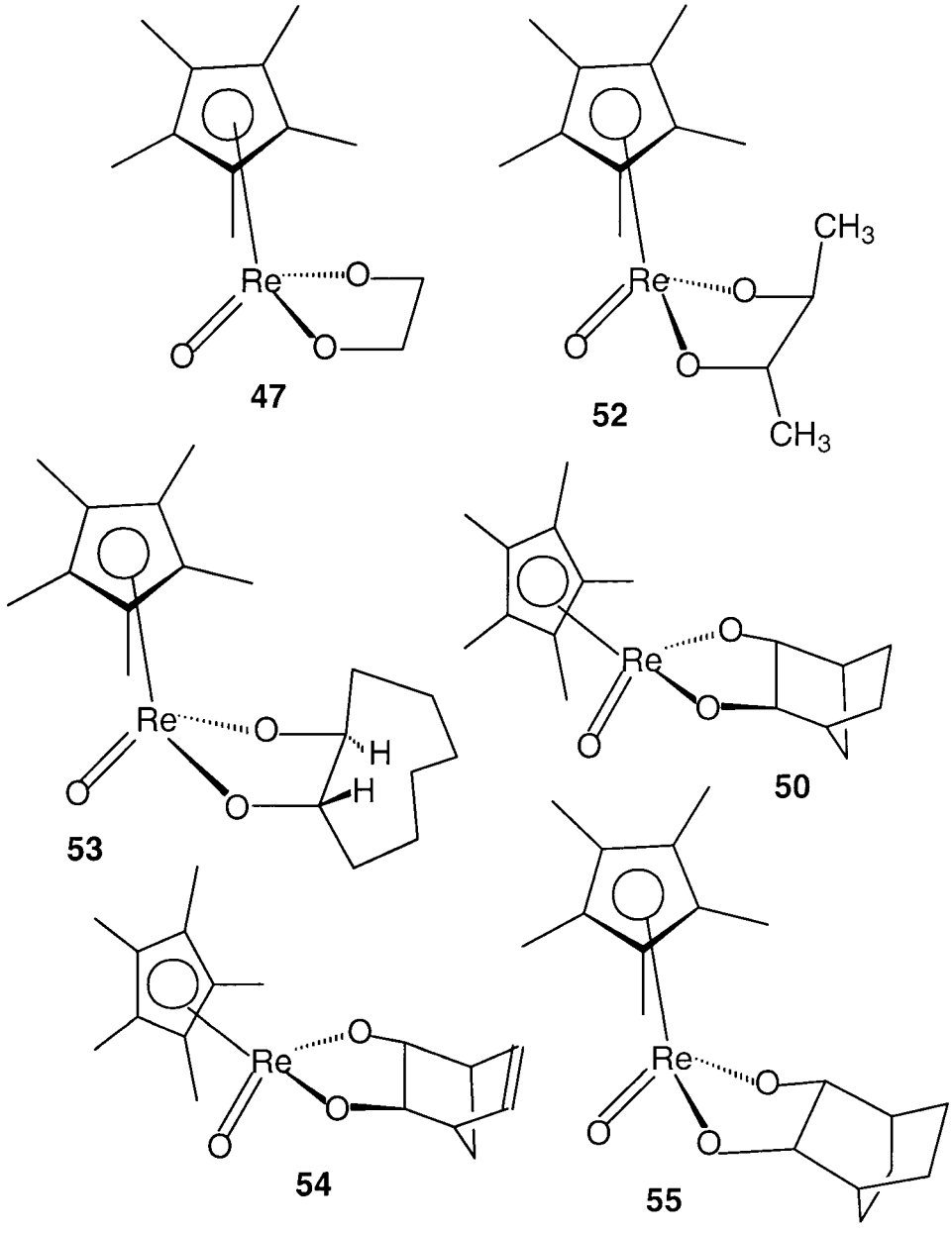

The strain on the double bond in the olefin has a predictable effect on the trend in the rate of extrusion; however, the degree to which the rate constants vary is not predicted based on a concerted mechanism. In Table 1.1, the rate of extrusion of strained norbornene from the Cp* rhenium diolate is smaller than the rate of extrusion of 2-butene. The rate constant for the oxidation process is likewise larger for strained olefins. For example, the rate constant for the oxidation of norbornadiene at 370.4 K is 7.20×10^{-5} $M^{-1}s^{-1}$, but the rate constant for oxidation of *trans*-cyclooctene at 370.4 K is 3.70×10^{-3} $M^{-1}s^{-1}$. This large difference in oxidation rate is strong evidence that the comparatively high strain of *trans*-cyclooctene is driving the reaction towards oxidation. A secondary deuterium kinetic isotope effect for ethylene extrusion was determined to be 1.32 ± 0.06 at 99.1 °C and 1.23 ± 0.06 at 104.8 °C.

The relationship of strain vs. rate and also enthalpy of activation noted above is more consistent with a stepwise process than with a concerted process. For the concerted mechanism, the enthalpy of activation for extrusion should increase with the strain energy. In fact, it does not seem to do this. Rather, the enthalpy of activation for extrusion is very similar for electronically comparable compounds regardless of strain. For example, the enthalpy of activation for extrusion of ethylene is 28.0 kcal/mol, while it is 29.1 kcal/mol for norbornene. The enthalpy of activation for oxidation should also be more affected by the strain of the olefin than the results show it to be. The difference between the enthalpy of activation for oxidation of norbornene and that of *trans*-cyclooctene is 6.5 kcal/mol, which is almost equal to the difference in strain energy. This means that the strain of each olefin is almost nonexistent in the transition state, and

Table 1.1: Selected Kinetic Data

Alkene	T, K	k_e X 10^5,s^{-1}	$\Delta H^{\ddagger}$ (kcal/mol)	$\Delta S^{\ddagger}$ (cal/molXK)
ethylene	372.2	12.5	28.0 ± 0.4	-2.1 ± 1.2
	378.0	21.6		
ethylene-d4	372.2	9.48		
	378.0	17.6		
2-butene	372.6	0.61	30.5 ± 0.5	-0.8 ± 1.1
	378.6	1.24		
norbornene	370.4	0.067,0.069	29.1 ± 0.5	-7.2 ± 1.8
	387.0	0.369		

therefore little sp^2 character exists in the transition state. The concerted transition state, if one did exist, would have to be diolate-like. A diolate-like transition state would not show the effects of strain as much because the double bond character would not be forming or disappearing at the transition state. But the diolate-like transition state ought to be similar in energy to the diolate by the Hammond postulate,[33] and it is not, as the enthalpy of activation values on the order of 30 kcal/mol indicate. The diolate-like transition state is also inconsistent with the kinetic isotope effect observed for the ethylene extrusions. An early transition state with little rearrangement of the diolate ought to have a very small secondary deuterium isotope effect. The per-deuterium isotope effect is actually 1.06-1.07 (assuming a concerted mechanism) which is quite substantial for a secondary deuterium isotope effect.

Hammett Studies

Another set of experiments by the Gable group that seemed to lend support to the stepwise mechanism were Hammett studies[34] involving substituted rhenium diolates. Linear free energy studies on substituted phenyl compounds can demonstrate whether the reaction is proceeding by a negative or positive charge build up or no charge build up at the transition state. If the plot of the logarithm of the rate constant vs. a certain σ is linear, then it becomes possible to draw some conclusions[35] about the transition state. The ρ value is the slope of this plot and is constant for a particular type of reaction–there is one ρ value for substituted benzoic acid ionization, another for hydrolysis of substituted ethyl benzoate, etc. There are four common types of σ parameters--σ^-, σ^+, σ_m, and σ_p. The σ^- values are used for reactions where there is a conjugated interaction between the substituent on the phenyl and an electron rich transition state. The σ^+ values are used for reactions in which the substituent on the phenyl is conjugated with an electron poor transition state. Therefore, if a linear k vs. σ plot results when the σ^+ value is used, then the reaction in question has an electron poor transition state which is interacting with the substituent on the phenyl ring. If a linear plot results from the use of σ^-, on the other hand, this is evidence that the reaction in question has an electron rich transition state that is in conjugation with the substituent on the phenyl ring. It is also possible to see no correlation if the transition state of the reaction is far away from the phenyl ring and its substituent. If a change in substituent induces a change in mechanism or a change in the global transition state in a multistep mechanism, the plots of ln k vs. σ are often curved[36] rather than linear.

The compounds used in the Hammett studies of the Gable group[37] include Cp* Re (O) phenylethanediolate and derivatives. The substituents on the phenyl group of these diolates included *p*-methoxy, *p*-methyl, *p*-flouro, *p*-chloro, *p*-triflouromethyl, and *m*-nitro. The plot of log k vs. σ for cycloreversion of the above compounds, where σ^- is used and $\rho = 0.42$, is linear with a positive slope. This is evidence for accumulation of electron density at the diolate carbon with the aromatic substituent. It is possible to assume that this is caused by an "asynchronous concerted" transition state (see Figure 1.18). However, there is other evidence that this explanation does not fit so well as a stepwise process. The intermediate would have to retain significant C-O interaction, otherwise the stereochemistry would not be retained. If there is an "asynchronous concerted" transition state that does in fact have the necessary C-O interaction, this would be unlikely to produce the large secondary kinetic isotope effect discussed previously. The isotope effect basically means that there is bond breakage during the transition state. The control of the electronics by using these substituents could have produced a curved Hammett plot due to differing rates of reaction for both steps such that for some of the Cp* Re (O) phenylethanediolates the first step would be faster than the second, and for others the second step faster than the first. More explicitly, the first bond to break in a stepwise extrusion mechanism could change with substituent. However, the plot for substituted styrenes is not curved, probably because the reaction at the benzylic position dominates in all cases. The Hammett plot for the extrusion of substituted stilbenes, however, is in fact curved. Since both bonds that break in the

Figure 1.18: Asynchronous Concerted Transition State

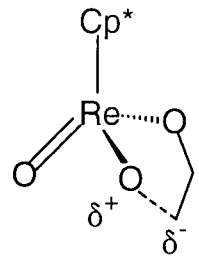

56

extrusion of substituted stilbenes are at the benzylic position, substituent effects can change which bond is broken first.

Solvent Effects on Cycloreversion of Rhenium Diolates

The effect of solvent on the extrusion of *p*-chlorostyrene from Cp* rhenium(oxo) *p*-chlorophenylethanediolate was also examined in this paper.[37] The observed rate constants were measured at 50.1 °C in benzene-d6, THF-d8, acetonitrile-d3, and acetone-d6. The largest observed rate constant was seen for the reaction in benzene-d6; it was (3.2 ± 0.3) X 10^{-5} s^{-1}. The smallest observed rate constant was seen for the reaction in acetone-d6; it was (2.8 ± 0.3) X 10^{-5} s^{-1}. The type of solvent seems to have very little effect on the rate of reaction. This, together with the ρ value of 0.42, suggest that something is occurring at the metal center during the rate determining step. The rate constants of styrene extrusion (from the Cp* rhenium diolate) were also measured and found to be very different from the rate constants of ethylene extrusion; at 323 K, the rate constant for extrusion of styrene is 2.0 X 10^{-5} s^{-1}, while the rate constant for

extrusion of ethylene is 2.6×10^{-7} s^{-1}. However, the rate constants at the same temperature for extrusion of Z-stilbene and E-stilbene respectively are 3.6×10^{-6} s^{-1} and 1.9×10^{-4} s^{-1}. Obviously, the rate of styrene extrusion and the rate of stilbene extrusion do not differ as much as the rate of ethylene extrusion and styrene extrusion. This is not what should happen if there is a transition state with significant sp^2 character; for a transition state that has much sp^2 character, the change from styrene to stilbene ought to have as dramatic a change in rate of extrusion as the change from ethylene to stilbene does.

Conformational Analysis Studies

Some of Gable's work centers around kinetics and conformational analysis of diolate cycloreversion.[38] The results of this study show that the average O-O dihedral angle of a given diolate has a linear influence on the entropy of activation. However, the results also show that in the case of the diolates of Z-2-butene and E-2-butene, the diolate with the most flat ring structure is the one that reacts most slowly. This is not what would be expected if the mechanism was concerted, since the geometry that would encourage formation of the [3+2] transition state is the flat ring.

Theoretical Work on the Comparison of Rhenium and Osmium

Recently, Frenking and Deubel[39] also reported that the [3+2] transition states seem to be lower in energy; however, this study also reported findings for the concerted and

stepwise transition states in the reaction of perrhenate, cyclopentadienyl rhenium trioxide and chloro rhenium trioxide. The energy barrier for the rearrangement of the metallaoxetane to the diolate was also determined. The calculations were done using Gaussian 94 at the B3LYP/II level. The basis set used for rhenium was a relativistic small-core ECP with a valence basis set splitting (441/2111/21). For all other atoms, the 6-31+G(d) basis set was used. For the donor-acceptor interaction of the [3+2] transition states, the charge decomposition analysis method (CDA, with the program CDA 2.1) was also used. In CDA, the Kohn-Sham orbitals are expressed in terms of linear combinations of the orbitals of the metal oxide and the ethylene. However, the CDA method does not apply to the formation of the [2+2] transition state. The relative energy of the [3+2] transition state, the [2+2] transition state, the metallaoxetane, and the diolate compared to the energy of the metal trioxide and ethylene was determined for osmium tetraoxide, perrhenate, chloro rhenium trioxide, cyclopentadienyl (Cp) rhenium trioxide, and pentamethylcyclopentadienyl (Cp*) rhenium trioxide.

However, the energy difference between the metallaoxetane and the diolate varies, not only with the compound investigated, but also with the method used.[39] For example, the difference between the energy of the [2+2] and [3+2] transition states for osmium tetraoxide was found to be 39 kcal/mol and 36.1 kcal/mol using the B3LYP/II and the B3LYP/III+//B3LYP/II method, respectively. The energies relative to the metal oxide and olefin of the diolate and the metallaoxetane for this compound using the B3LYP/II method are -32.3 kcal/mol and +5.0 kcal/mol, respectively. For the B3LYP/III+//B3LYPII method, the relative energy values for the diolate and the

metallaoxetane are -19.1 kcal/mol and +12.7 kcal/mol. The relative energies of the diolate and metallaoxetane (for osmium tetraoxide) calculated at the CCSD(T)/II//B3LYP/II level are -21.2 kcal/mol and +11.1 kcal/mol. Thus, no matter which level the calculation was done at, the basic conclusion is that the metallaoxetane is higher in energy than the diolate. The results for the rhenium oxides also show this pattern, but except for the cyclopentadienyl rhenium oxides, where this difference is about 10 kcal/mol, there is an energy difference on the order of 1-4 kcal/mol between the metallaoxetane and the diolate, while this difference for the osmium tetraoxide is on the order of 30-40 kcal/mol.

Frenking[39] also found the difference between the relative transition state energies; these are also found to be smaller for the rhenium oxides than for osmium tetraoxide. The [3+2] transition state energy relative to metal oxide and olefin for the B3LYP/II method is 5.0 kcal/mol for osmium tetraoxide, 21.8 kcal/mol for chloro rhenium trioxide, and 13.6 kcal/mol for Cp rhenium trioxide. The relative energies of the [2+2] transition state at the same level of calculation are 44.0 kcal/mol for osmium tetraoxide, 30.0 kcal/mol for chloro rhenium trioxide, and 25.4 kcal/mol for $CpReO_3$. Basically, the differences between the relative energies of the [2+2] transition state and the [3+2] transition state for the different levels of calculation for osmium tetraoxide are on the order of 30-40 kcal/mol, while these same differences for the rhenium oxides are on the order of 10-20 kcal/mol. The transition state for rearrangement of the metallaoxetane to the diolate was found to have a very high relative energy in all cases as well. For example, the energy relative to the metal oxides and olefin of this transition state for

osmium tetraoxide at the B3LYP/II level of theory is 36.2 kcal/mol. At the same level of theory, this energy is 52.2 kcal/mol for chloro rhenium trioxide. The barrier to rearrangement is found to be higher for the rhenium oxides, when it is between about 49 kcal/mol and 110 kcal/mol, than for osmium tetraoxide, when it is between about 36 kcal/mol and 48 kcal/mol.

The general result is that the transition state for the concerted process in all cases is predicted to be lower in energy than the transition state for the stepwise process, and the energy of rearrangement of the metallaoxetane to the diolate is very high. The energy of the metallaoxetane is also in all cases higher than the energy of the diolate. The authors[39] conclude that the [3+2] concerted reaction is in all cases a lower energy pathway, but concede that the energy difference is not as great for rhenium oxides as for osmium tetraoxide. However, they also claim that the rearrangement of the metallaoxetane to form the diolate has too high an activation barrier to be feasible, so they also support a concerted mechanism for the reaction of rhenium oxides with olefins.

Conclusions of the Literature Review

The conclusion of the concerted vs. stepwise mechanism debate is still undecided. The curvature of the Eyring plots that Sharpless found seem to indicate that the stepwise mechanism is operating, but this cannot rule out a concerted mechanism. The more recent computational work favors a concerted mechanism, but there are conflicting studies which favor a stepwise mechanism. The specific stereochemistry of the products in the asymmetric dihydroxylation seems to favor a stepwise mechanism, but this again

fails to rule out a concerted mechanism. The experimental work with rhenium diolates, including conformational, Hammett, and other work, seems to indicate that the stepwise mechanism is the one which best fits the data.

Chapter 2. Experimental Design and Results

Review of Cycloreversion of Rhenium Diolates

None of the evidence involving direct study of the osmium tetraoxide oxidation mechanism is conclusive, so studying similar reactions involving a different transition metal might prove fruitful. Rhenium diolates undergo cycloreversion when heated (Figure 2.1);[40] this is formally the reverse reaction of the osmium tetraoxide oxidation. The principle of microscopic reversibility is the theory that the same pathway that is traveled in the forward direction of a reaction as will be traveled in the reverse reaction.[41] This conclusion arises from transition state theory because according to this, the path of the reaction is the minimum energy pathway and should therefore be taken when products return to reactants as well as when reactants become products. By this principle then, the mechanism of cycloreversion of rhenium diolates can shed light on

Figure 2.1: Cycloreversion of a Tp' Complex

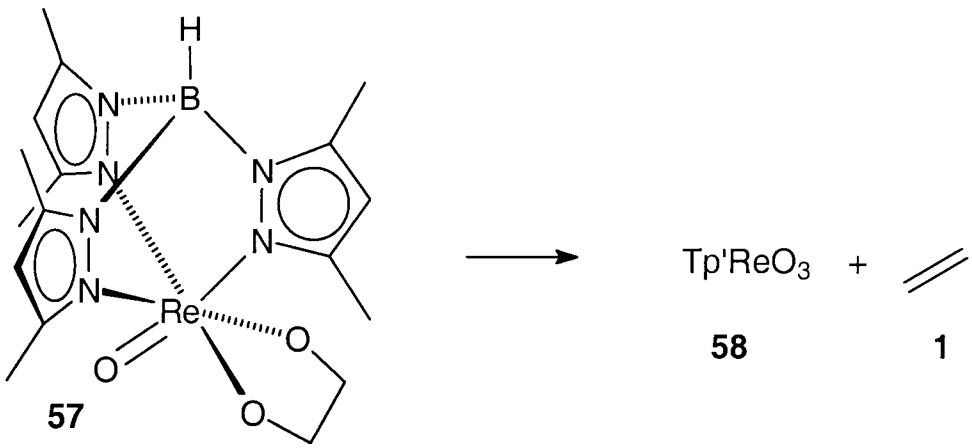

the osmium tetraoxide oxidation of olefins. Rhenium is a group 7 transition metal and was therefore expected to do some kind of oxidation chemistry, since tungsten (group 6) and osmium (group 8) do oxidation chemistry. The cycloreversion of rhenium diolates is a much slower reaction than the osmium tetraoxide oxidation, and might therefore be expected to be easier to study.[29]

Design of ^{18}O Labeling Experiment

The experiment designed to study the mechanism of cycloreversion (Figure 2.2) involved making an oxygen-18 labeled diolate that could not undergo net cycloreversion because of thermodynamics. Then when this diolate was heated, the intermediate towards cycloreversion would presumably form but would collapse to form the diolate again. If the process were a stepwise one, it is likely that the oxygen-18 would move into (or out of) one diolate position more than the other diolate position. If, however, the oxygen-18 migrated into (or out of) both diolate oxo positions at the same rate, this would indicate a concerted intermediate provided the two diolate oxo positions were not chemically identical. The diolate chosen for this experiment was tris-(3,5-dimethylpyrazolyl)-hydridoboratorhenium (V) (oxo)*trans*-1,2-cyclooctanediolate (Tp'Re(O)*trans*-1,2-cyclooctanediolate). This diolate will not undergo net cycloreversion because of the relative instability of the *trans*-cyclooctene. The diolate oxo positions are also chemically different, or diastereotopic, from each other–if they were not diastereotopic, the stepwise process would show no difference in C-O bond breakage at the two positions.

Figure 2.2: Migration of Oxygen-18

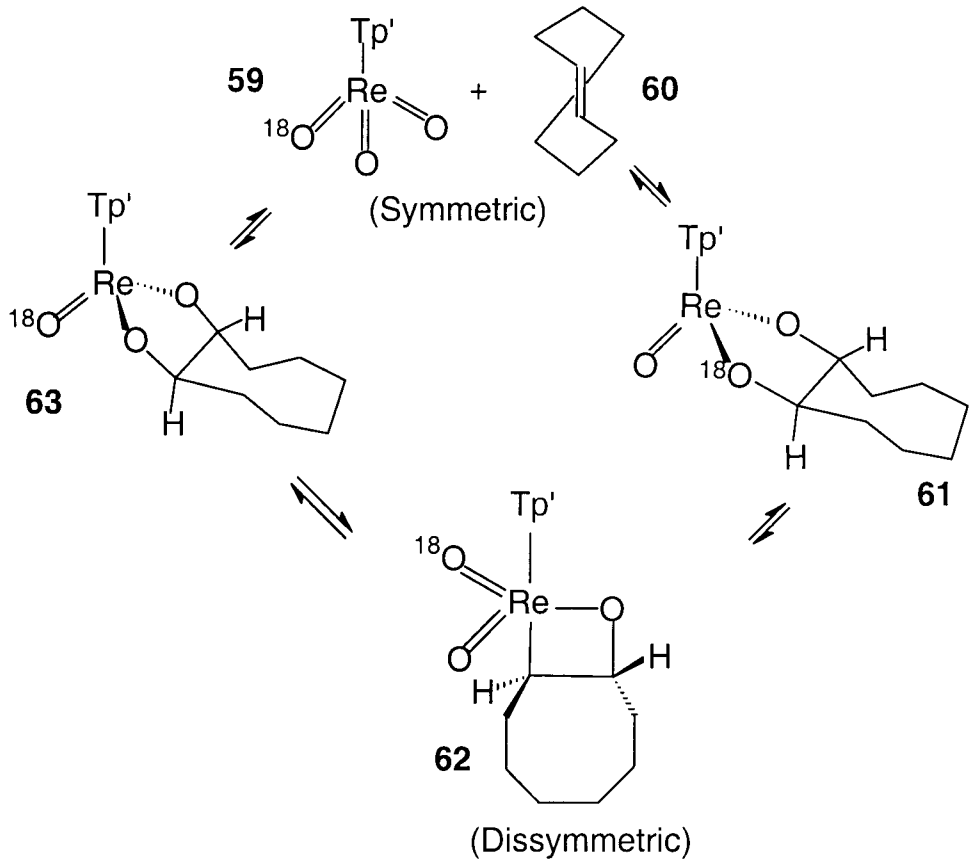

Synthesis and Characterization of Unlabeled Diolate

The unlabeled diolate was synthesized according to previous methodology.[42] The synthesis is shown in Figure 2.3. After filtration and solvent removal, the product was purified by recrystallization from ethanol/water or by column chromatography using chloroform to elute the diolate. The diol could be eluted after this with ethyl acetate.

Figure 2.3: Synthesis of Diolate Complex

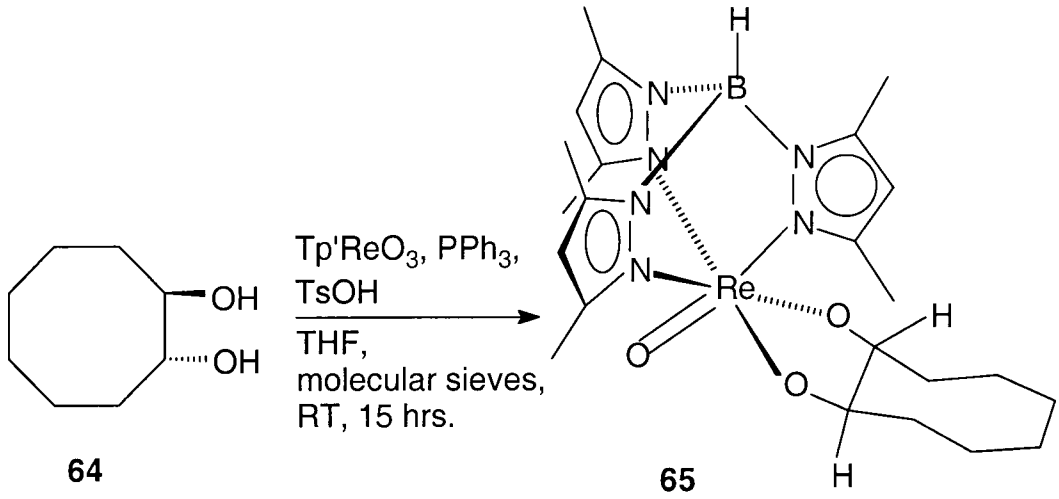

The unlabeled diolate was characterized by means of ^{1}H NMR, ^{13}C NMR, COSY, NOE, and HETCOR experiments. The NMR assignments are shown in Figures 2.4 and 2.6. NOE experiments on the Tp'Re(O)*trans*-1,2-cyclooctanediolate were done in order to give definitive assignments for the two diolate position hydrogens, which could then be used to give definitive assignments to all of the hydrogens of the ring except those on the two distal carbons. NOE experiments (see Figure 2.5) were done in order to definitively assign the signals of the two diolate hydrogens. Irradiation of the signal at 2.51 ppm gave a 3.54% NOE effect at the 5.22 ppm signal and a 7.94% effect at the 5.68 ppm signal. Therefore, the methyl signal on the Tp' ligand shows both an NOE for the aromatic hydrogen next to it (5.22 ppm) and for the diolate hydrogen at 5.68 ppm.

Figure 2.4: Proton Assignments

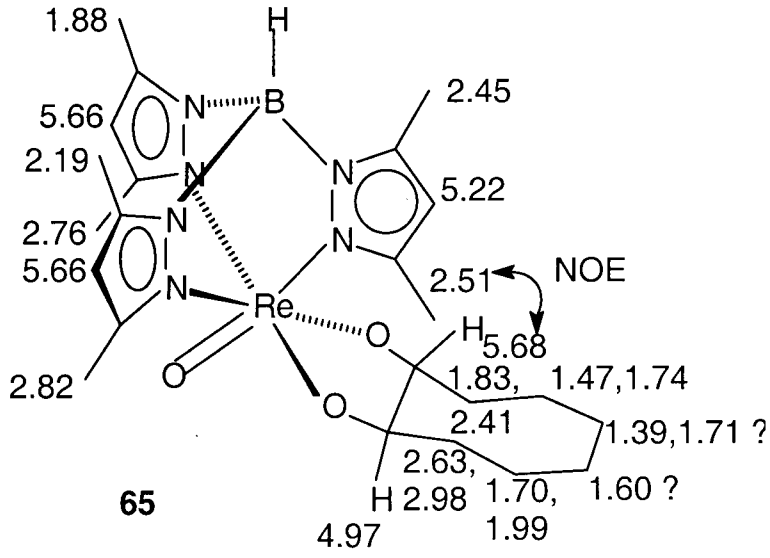

(Chemical shifts in benzene-d6.)

Irradiation of the methyl signal at 2.19 ppm gave a 10.38% effect at the 5.68 ppm signal, and irradiation of the methyl signal at 2.76 ppm gave a 4.19% NOE effect at the 5.68 ppm signal. However, these results are not as clear, since the aromatic hydrogens near these two methyl groups have signals of about 5.66 ppm, which is difficult to distinguish from 5.68 ppm.

The COSY spectrum (Figure 2.7) allowed for the assignment of all of the signals in the eight membered ring except those for the four hydrogens on the two distal carbons. For example, the coupling between the signal at 4.97 ppm and the signals at 2.98 ppm and 2.63 ppm allowed those signals to be assigned to the hydrogens next to the hydrogen

Figure 2.5: NOE Spectrum of Tp'Re(O)*trans*-1,2-cyclooctanediolate

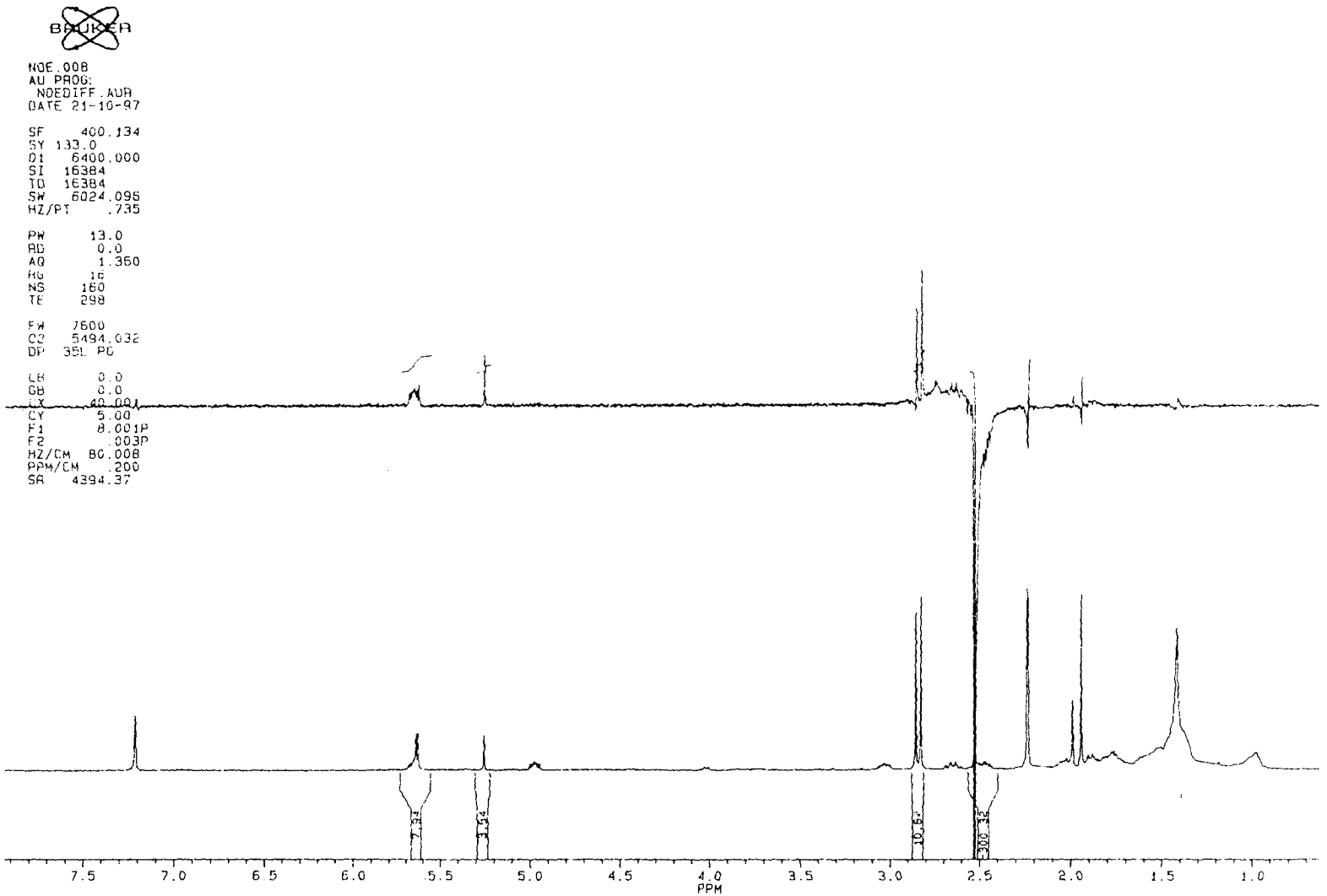

at 4.97 ppm. The HETCOR experiment (Figure 2.8) allowed the carbon signals to be definitively assigned to the proton signals, and also confirmed that the two diolate carbon signals were far enough apart to make this experiment possible.

Figure 2.6: ^{13}C Assignments

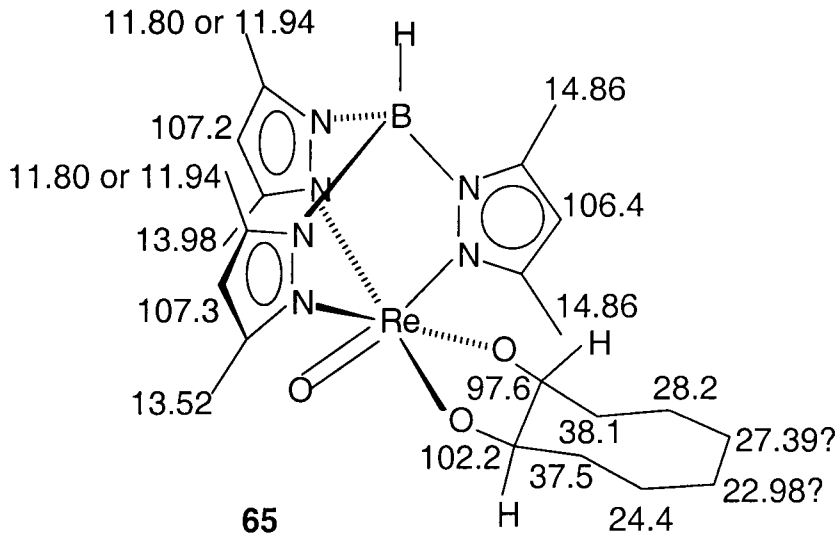

65

(Chemical shifts in benzene-d6.)

Attempted Synthesis of Labeled Compound with ^{18}O in the Oxo Position

The synthesis of the oxygen-18 labeled diolate began with attempts to place the oxygen-18 label in the terminal oxo position. Considerable effort was invested in making the Tp'$ReOCl_2$, since this could then be used to make the Tp'ReO_2 , with one of the two oxygens being oxygen-18. The synthesis of the labeled diolate from this

Figure 2.7: COSY Spectrum of Tp'Re(O)*trans*-1,2-cyclooctanediolate

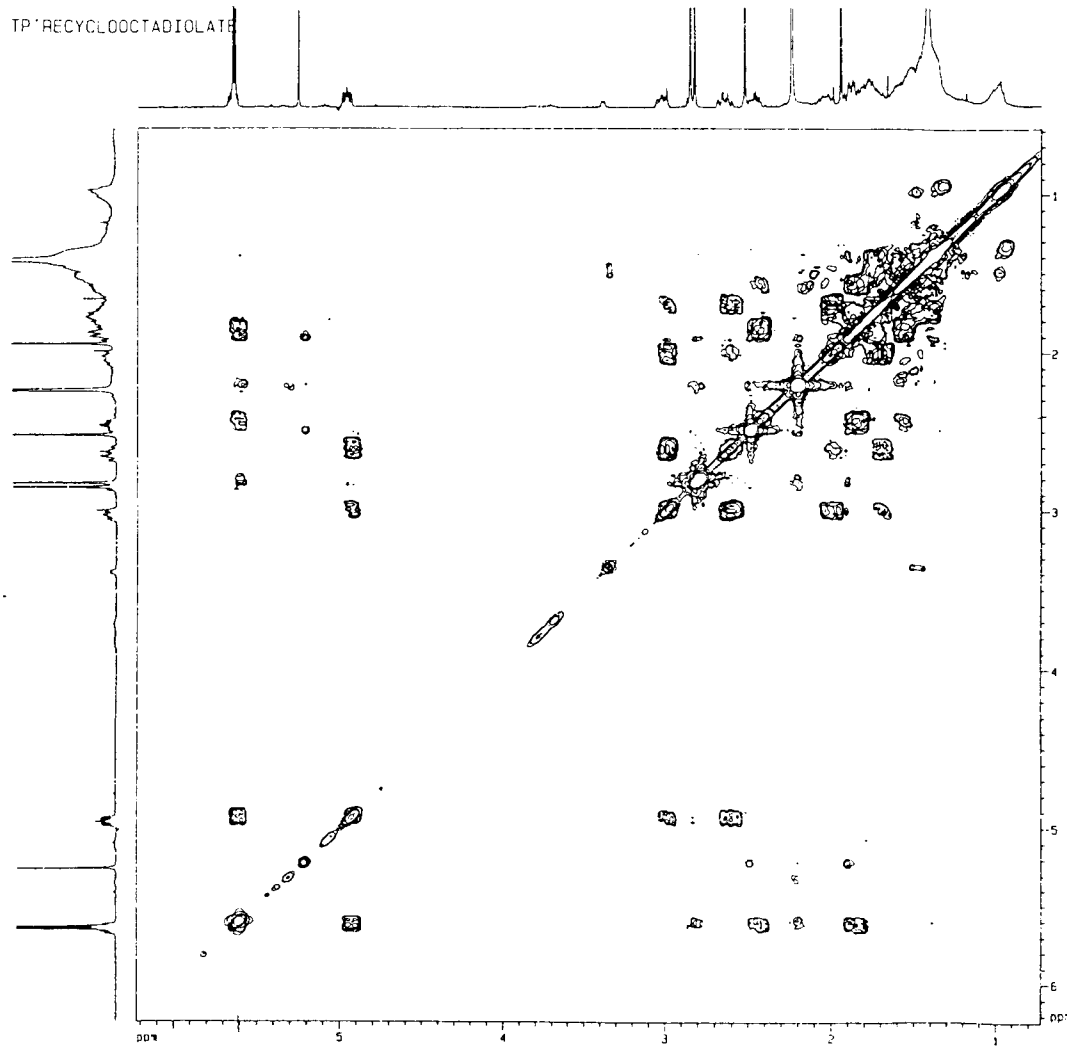

Figure 2.8: HETCOR Spectrum of Tp'Re(O)*trans*-1,2-cyclooctanediolate

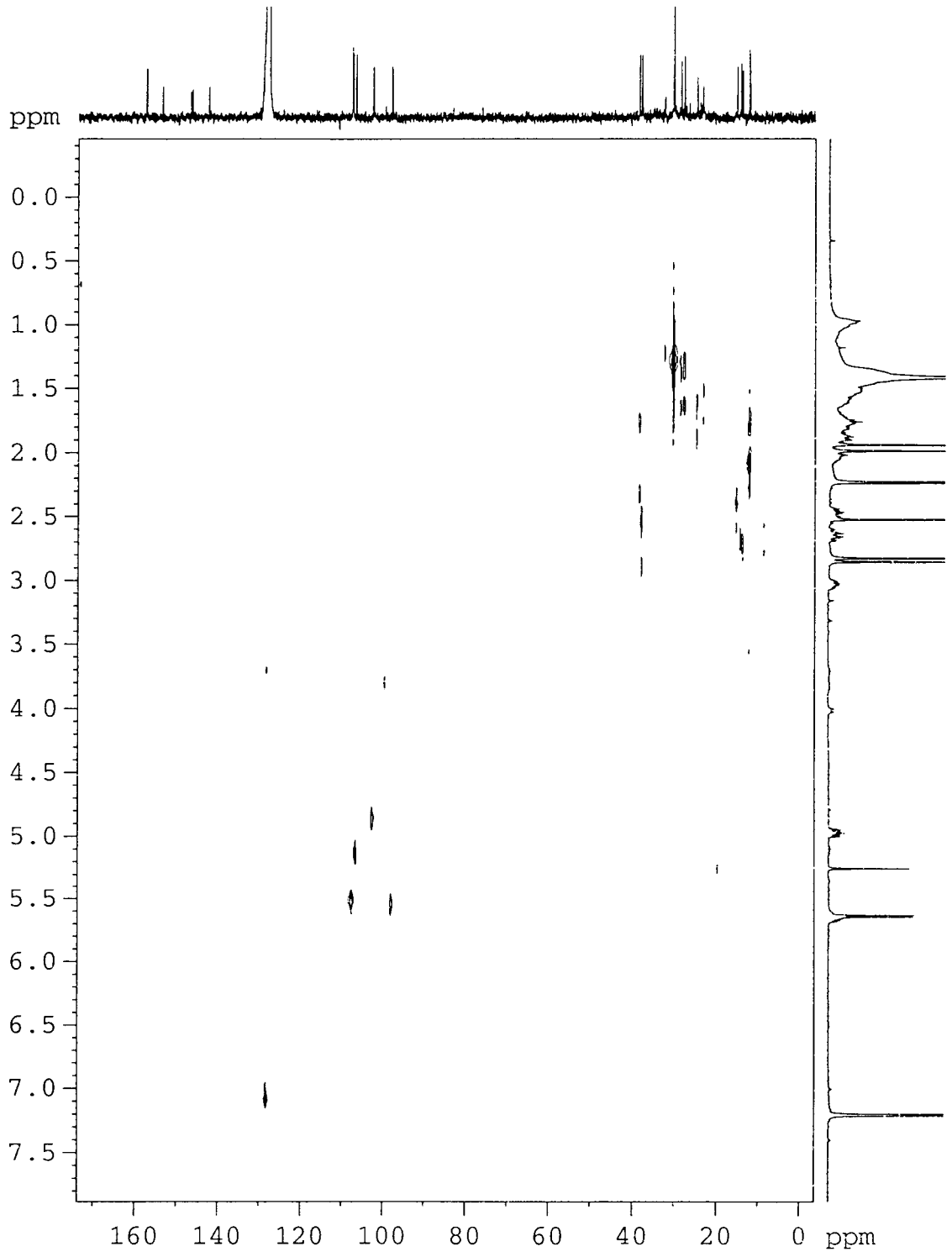

compound was thought to be relatively straightforward. One method of synthesis, based on Santos' synthesis[43] of the corresponding oxo dichloride of the tetrakispyrazolylborate, involved reduction of the trioxide with triphenylphosphine in the presence of TMSCl (Figure 2.9). This method was relatively unsuccessful–on one occasion a distinct color change from brown to green-blue took place, but as the compound was hexane soluble, it could not be purified from the triphenylphosphine. Coe used similar methodology[44] and synthesized an inseparable mixture of Tp'$ReOCl_2$ and Tp'ReO(OH)Cl. Another method of synthesis, which was taken from Mayer's synthesis of $TpReOCl_2$, was equally unsuccessful. This synthesis used $KReO_4$ as the rhenium source and is discussed in more detail below. This reaction was totally unproductive, as the compound it generated was a dimeric complex[45] instead of the oxo dichloride.

Figure 2.9: Proposed Synthesis of Tp'$ReOCl_2$

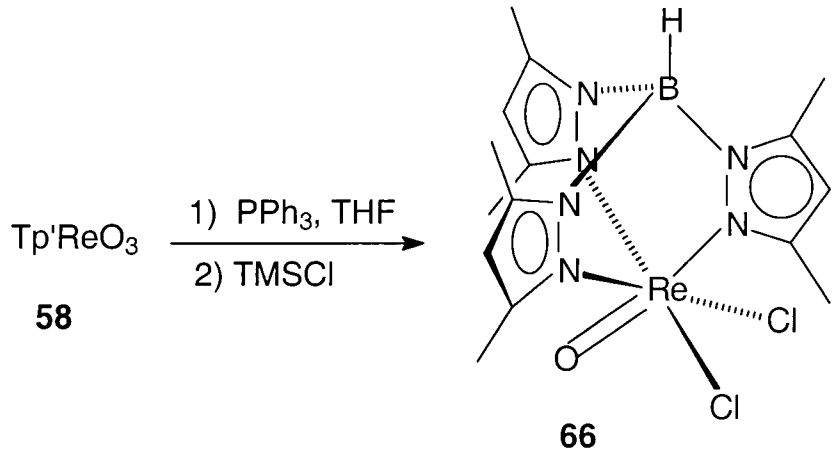

Attempts to Synthesize ^{18}O Labeled Cyclooctanediol

Since attempts to place the oxygen-18 on the terminal oxo position were unsuccessful, the plans for the experiment were slightly altered. Instead of monitoring movement of oxygen-18 into the diolate oxo positions, the plan was now to place the oxygen-18 in the diolate positions and monitor movement of oxygen-18 out of the diolate positions. To this end, the labeled *trans*-1,2-cyclooctanediol was synthesized.[46] The first attempt to do this involved basic hydrolysis (Figure 2.10) . It was hoped that this would yield exclusively the *trans* product. However, the reaction did not produce anything–not even after 7 days at 123°C. It is interesting that none of the alternative expected elimination product, 2-cyclooctenol, was seen. This is believed to be the result of the boat-twist chair conformation of the cyclooctene oxide (see Figure 2.11). This conformation prevents both attack of the nucleophile at the epoxide and alignment of O-H with C-O required for eliminative ring opening. Another group reported in the literature that the basic hydrolysis of this particular epoxide is slow.[47]

Acid hydrolysis of cyclooctene oxide was then tried, and this was finally successful. Several different conditions were compared (Figure 2.12). The first was 0.81 N H_2SO_4 at RT in DMSO-d6/D_2O(75/25)–the NMR tube reaction was complete within 12 hrs. The next NMR tube reaction was run in the same solvent system and acid but with 0.01 M of H_2SO_4 at 35°C for 3 days. In the ^1H NMR spectra, the *trans*-1,2- cyclooctanediol hydrogens that are proximate to the hydroxy groups are found at about 3.3 ppm, whereas the equivalent hydrogens for the *cis* diol are found at about 3.6 ppm. By integration of these peaks and comparison of their relative values, it was found that both of the above

Figure 2.10: Basic Conditions for Synthesis of Diol

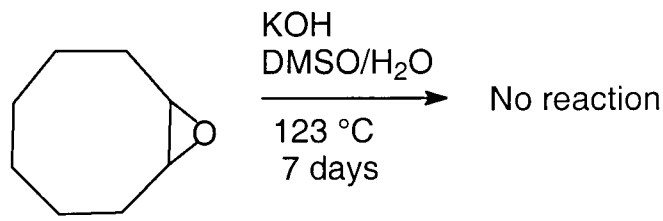

67

Figure 2.11: Boat-Twist Chair Conformation of Cyclooctene Oxide

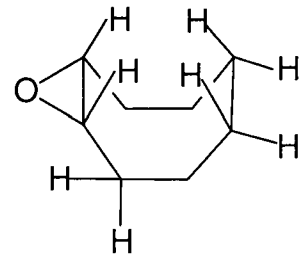

67

conditions gave a *trans*:*cis* ratio of 9:1. The hydrolysis was also tried using the same solvent system and *p*-toluenesulfonic acid. However, this reaction gave a *trans*:*cis* ratio of 6:4. Therefore, the large scale synthesis of *trans*-1,2-cyclooctanediol was done using 0.01 N H_2SO_4 in 7.3 mL of DMSO and 2.0 mL of water. After heating with stirring for 5 days at 35°C, the mixture was extracted with chloroform to remove diol and DMSO. The chloroform was then extracted with water to remove most of the DMSO. The remaining DMSO was removed when the diol was purified by silica gel column chromatography using ethyl acetate to elute the diol quite rapidly.

Figure 2.12: Acidic Conditions for Synthesis of Diol

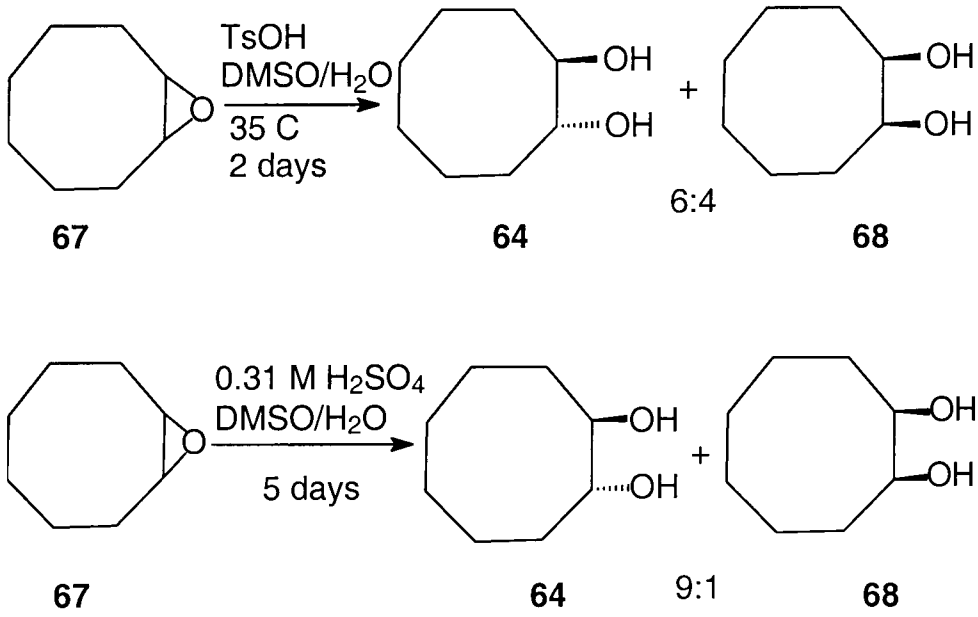

Synthesis of ^{18}O Labeled Diolate

The synthesis of the oxygen-18 labeled *trans*-1,2-cyclooctanediol was done using the same method described for the unlabeled diol synthesis above, with the exception that the water was $H_2{}^{18}O$. The ^{13}C NMR of this labeled diol (Figure 2.13) had one small peak about 2 hertz upfield from the most downfield main peak at 76.11 ppm. This small peak was shifted away from the main peak because the carbon oxygen bond frequency is lower if the oxygen is oxygen-18. As determined by integration of the two peaks, the amount of diol with oxygen-18 was only about 18.7%. If one assumed total exchange with all of the oxygen atoms in sulfuric acid, this should have given an incorporation of oxygen-18 into the *trans*-1,2-cyclooctanediol of about 76%. The most

Figure 2.13: ^{13}C NMR Spectrum of ^{18}O Labeled *trans*-1,2-cyclooctanediol

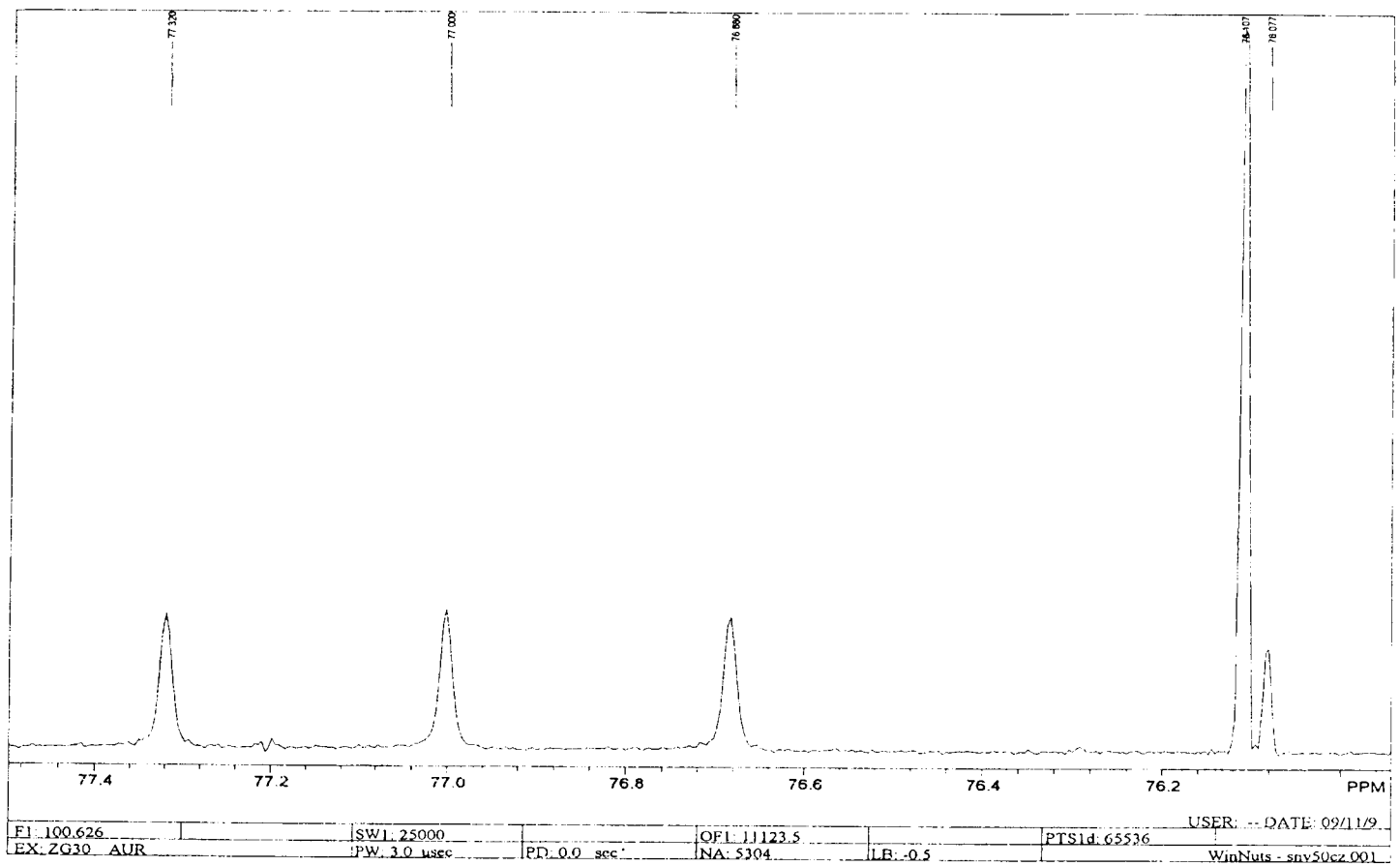

likely explanation for the low incorporation of oxygen-18 is that the oxygen molecules of the DMSO also exchanged.

The labeled Tp'Re(O)*trans*-1,2-cyclooctanediolate was synthesized in the same manner as the unlabeled diolate. However, one modification that was made was the addition of only 0.2 equivalents of *p*-toluenesulfonic acid instead of a full equivalent. This modification appeared to increase the rate and extent of reaction, for the color change took place more rapidly. The reaction mixture was the same bluish-beige color after 5 hours at room temperature as the reaction with a full equivalent of *p*-toluenesulfonic acid had been after 15 hours at room temperature. After 15 hours at room temperature, the reaction mixture was a brilliant royal blue. The mixture was filtered and stripped of THF under vacuum as before, and then it was purified by column chromatography using chloroform to elute the diolate. The diolate came off of the column very slowly. There was also some blue material that appeared to be diolate that came off with a mixture of ethyl acetate and chloroform; unfortunately this was contaminated with an unidentified green substance that may be a decomposition product. The yield after chromatography was 49%. This is a very good yield for this process, especially considering that the contaminated material was not included in the calculation. The unreacted labeled *trans*-1,2-cyclooctanediol was then removed from the column with ethyl acetate.

Characterization of the ^{18}O Labeled Diolate

The labeled Tp' Re (O) *trans*-1,2-cyclooctanediolate was characterized by ^{1}H NMR and mass spectroscopy. The ^{1}H NMR spectrum of this compound is identical with the spectrum obtained for the unlabeled material. The identity of the compound was thus established beyond a reasonable doubt. However, the percentage of oxygen-18 incorporation was still not known. In order to determine this, a mass spectrum for the labeled diolate and one for the unlabeled diolate were obtained. The ideal mass spectrum for this compound was also calculated from isotopic natural abundances using the Sheffield Chemputer.[48] The peak intensities for the peaks in the region of the compound's molecular mass, which is 640-642 g/mol, for the spectrum of the unlabeled diolate, the spectrum of the labeled diolate, and the calculated ideal spectrum were entered into a spreadsheet program. A linear regression was then done using the unlabeled diolate intensities as the dependent variable and the ideal intensities for the unlabeled diolate as well as the ideal intensities for the pure labeled diolate (which is determined at each mass by using the ideal intensity of unlabeled diolate from a mass that is two units below the mass for labeled diolate) as the independent variables. A second linear regression was done using the labeled diolate intensities as the dependent variable and both the calculated ideal intensities of the unlabeled diolate and the ideal intensities of the pure labeled diolate as the independent variables. The coefficients for the independent variables in this second linear regression were proportional to the percentages of unlabeled and labeled diolate. The first linear regression was done in order to check the method; since it shows that the unlabeled diolate has virtually no

oxygen-18 in it, the method is probably sound. The amount of oxygen-18 labeled diolate in the labeled material that was synthesized was calculated to be 19.2 ± 2.2 %. The sample size was 12, there were 9 degrees of freedom, and R^2=0.9916.

NMR Solvent Studies

The ^{13}C NMR signals corresponding to the diolate carbons (at about 97 and 102 ppm in benzene-d6) were broad. Since narrow line shapes would aid detection of ^{18}O shifted signals, many experiments were done in an attempt to narrow the lines. Heat caused the lines to broaden; cold temperatures that were tried had the same effect. Increasing the field strength also broadened the signals. The solvents that were investigated were benzene-d6, chloroform-d, and acetone-d6. The solvent that broadened the signals the most was chloroform-d; this was also the solvent that gave the best signal-noise-ratio, as the Tp' rhenium(oxo) *trans*-1,2-cyclooctanediolate had the highest solubility in it. The Tp' rhenium(oxo) *trans*-1,2-cyclooctanediolate had the lowest solubility in acetone-d6, but also the narrowest line shape in this solvent. Because of this, a mixture of 4:1 acetone-d6 and chloroform-d was used to give the best compromise between resolution and signal-to-noise ratio.

Pyrolysis of ^{18}O Labeled Diolate

The oxygen-18 labeled Tp'Re(O)*trans*-1,2-cyclooctanediolate was then dissolved in toluene-d8 and sealed into 7 NMR tubes under vacuum. The tubes were then heated at

106.1 ± 0.5 °C for 0.5 hours, 1 hour, 2 hours, 5 hours, 10 hours, 30 hours, and 72 hours. These times were chosen because the goal was to get at least a couple of samples at one half-life of the reaction which, as mentioned above, would be simply formation of the transition state for the cycloreversion followed by a rearrangement back to the diolate. Therefore, the rate of cycloreversion of Tp' rhenium(oxo)*cis*-1,2-cyclooctanediolate was taken as the upper limit for the rate of reaction, and the rate of cycloreversion of Tp' rhenium(oxo)ethanediolate was taken as the lower limit for the rate. Using the Eyring equation and available free energies of activation, the half-life for the upper limit at 106 °C was found to be 20 minutes, while the half-life for the lower limit at the same temperature was found to be 65 hours. The seven incubation times were chosen so that the half-life, which would be the time when the oxygen-18 label would have started to move out of one or both diolate positions, would be close to the reaction time. If the diolate were heated for a significantly longer period of time than the half life, the oxygen-18 label would become equally distributed amongst the three oxygen positions, no matter what the mechanism of rearrangement was. In order to test the hypothesis that such scrambling would take place, an eighth tube was prepared and heated at 105.6 ± 0.5 °C for 2 weeks. Unfortunately, this experiment caused the diolate to decompose, as the color change from blue to green indicated; nevertheless the ^{1}H NMR of this sample showed no significant change had occurred.

The NMR tubes were removed from the oil bath, cracked open, and the toluene-d8 stripped off under vacuum. The diolate was then dissolved in a 4:1 mixture of acetone-d6/ chloroform-d and sealed into NMR tubes under vacuum. The acetone/chloroform

mixture was found to give a narrow line shape of the carbon signals at about 97 ppm and 102 ppm and good signal to noise ratio. The DEPT ^{13}C NMR spectrum was taken of each tube overnight, thermostated at 298 K. Temperature regulation was important because the diolate spectrum has peaks which broaden with increasing or decreasing temperature. The peaks at about 97 ppm and 102 ppm were examined carefully, and the height of the shoulder about 2 hertz upfield from each peak relative to the height of the peak was determined. The shoulder is the signal shifted because of the carbon's attachment to oxygen-18. The shoulder to peak ratio for both peaks for a sample of the diolate that was not heated was about 0.27. This means that at the start of the experiment, the amount of oxygen-18 in the two diolate positions was equal. However, the shoulder to peak ratios for the samples heated for 30 hours and 72 hours were different, as can be seen in Table 2.1. This implies movement of oxygen-18 from one diolate position preferentially. (Spectra are shown in Figures 2.14-2.17.)

Table 2.1: Ratio of Labeled vs. Unlabeled Oxygen in the Diolate Position at Different Heating Times

Time heated	shoulder/peak height at102 ppm	shoulder/peak height at 97 ppm
0 hours	0.27	0.27
10 hours	0.22	0.18
30 hours	0.27	0.16
72 hours	0.27	0.11

Figure 2.14: Spectra of ^{18}O Labeled Tp'Re(O)*trans*-1,2-cyclooctanediolate at Time 0 hrs.

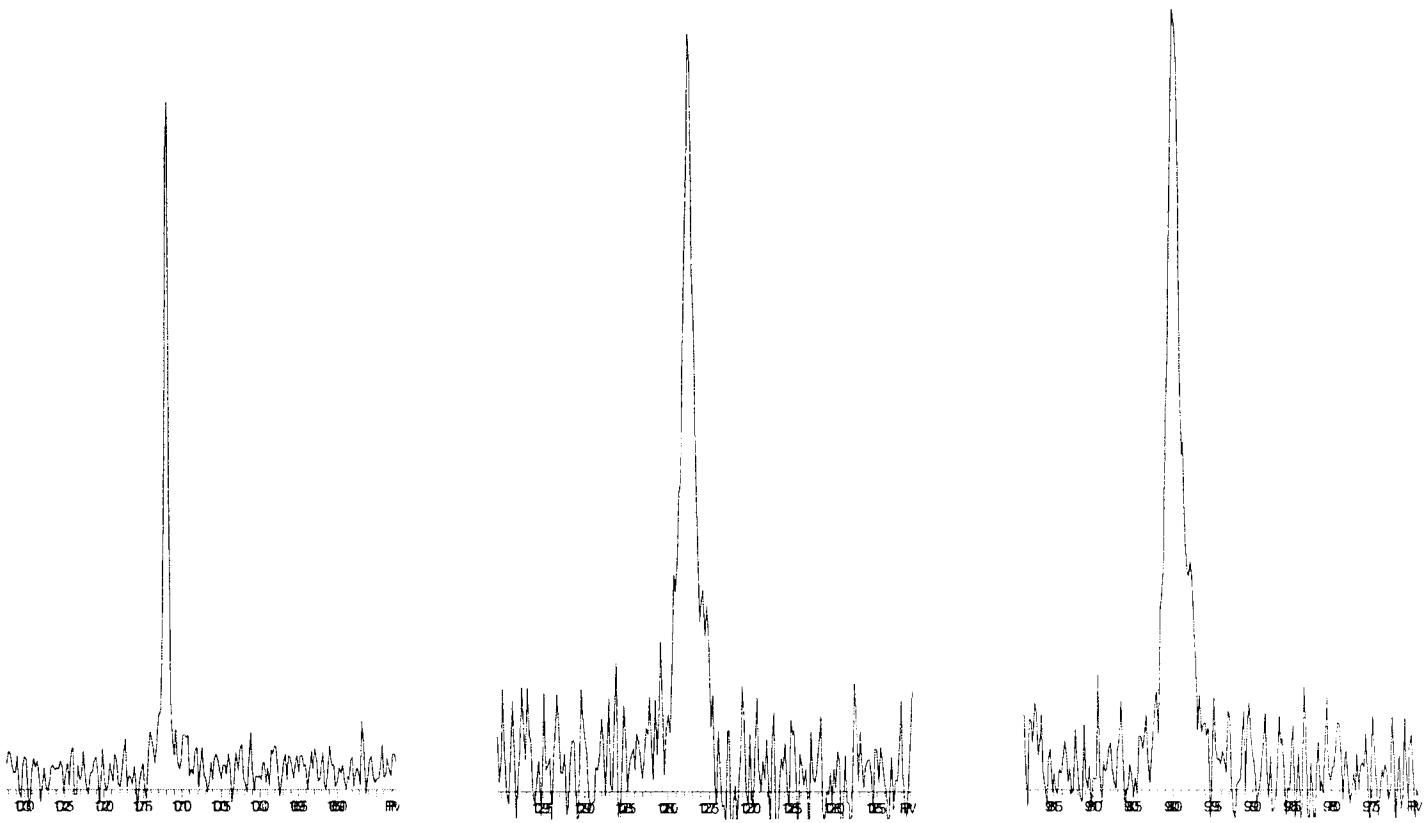

Line shape reference
107.1 (Tp' Vinyl)

102.8

98.0

Figure 2.15: Spectra of ^{18}O Labeled Tp'Re(O)*trans*-1,2-cyclooctanediolate After Heating for 30 hrs.

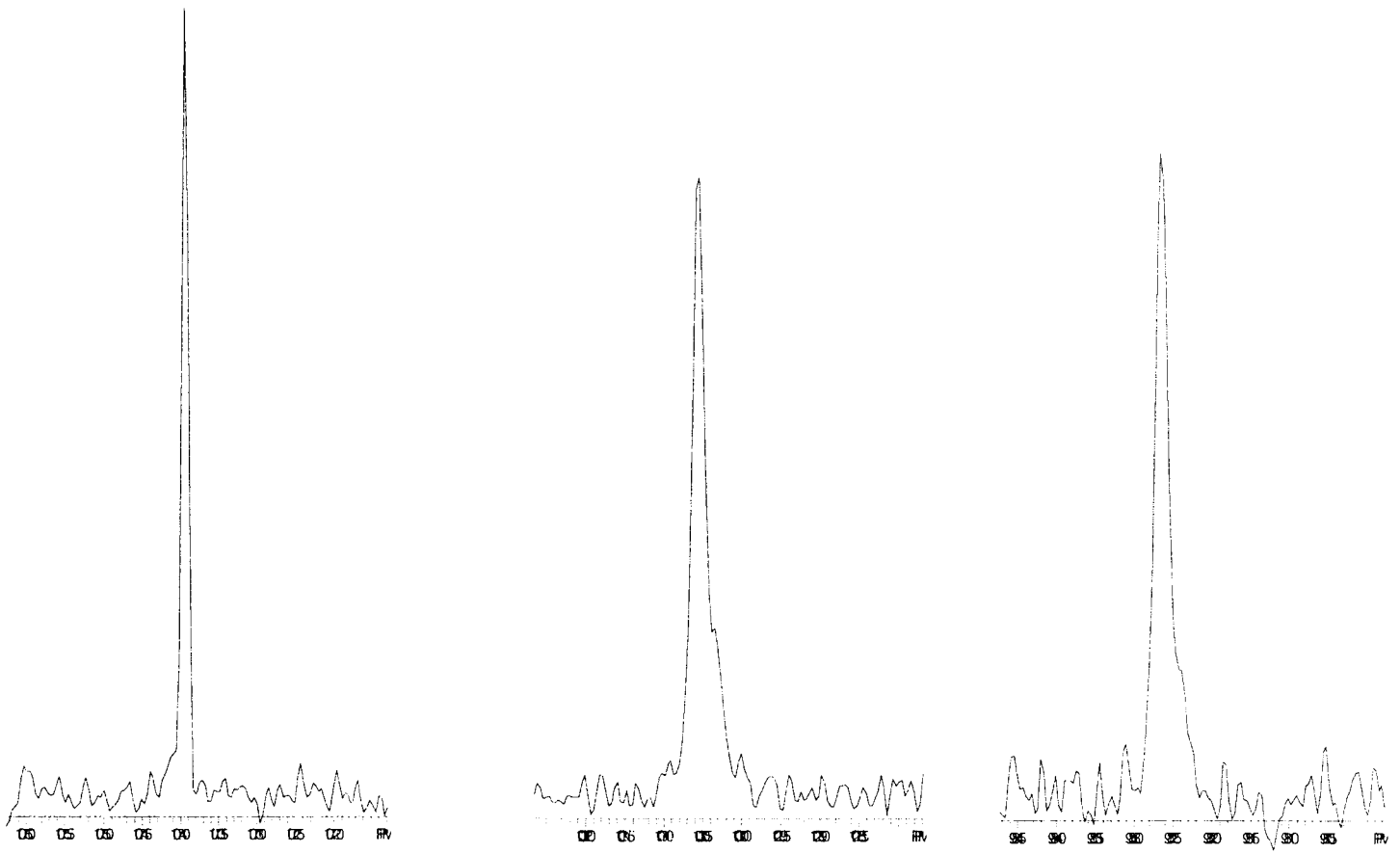

Line shape reference
107.1 (Tp' Vinyl)

102.8

98.0

Figure 2.16: Spectra of ^{18}O Labeled Tp'Re(O)*trans*-1,2-cyclooctanediolate After Heating for 72 hrs.

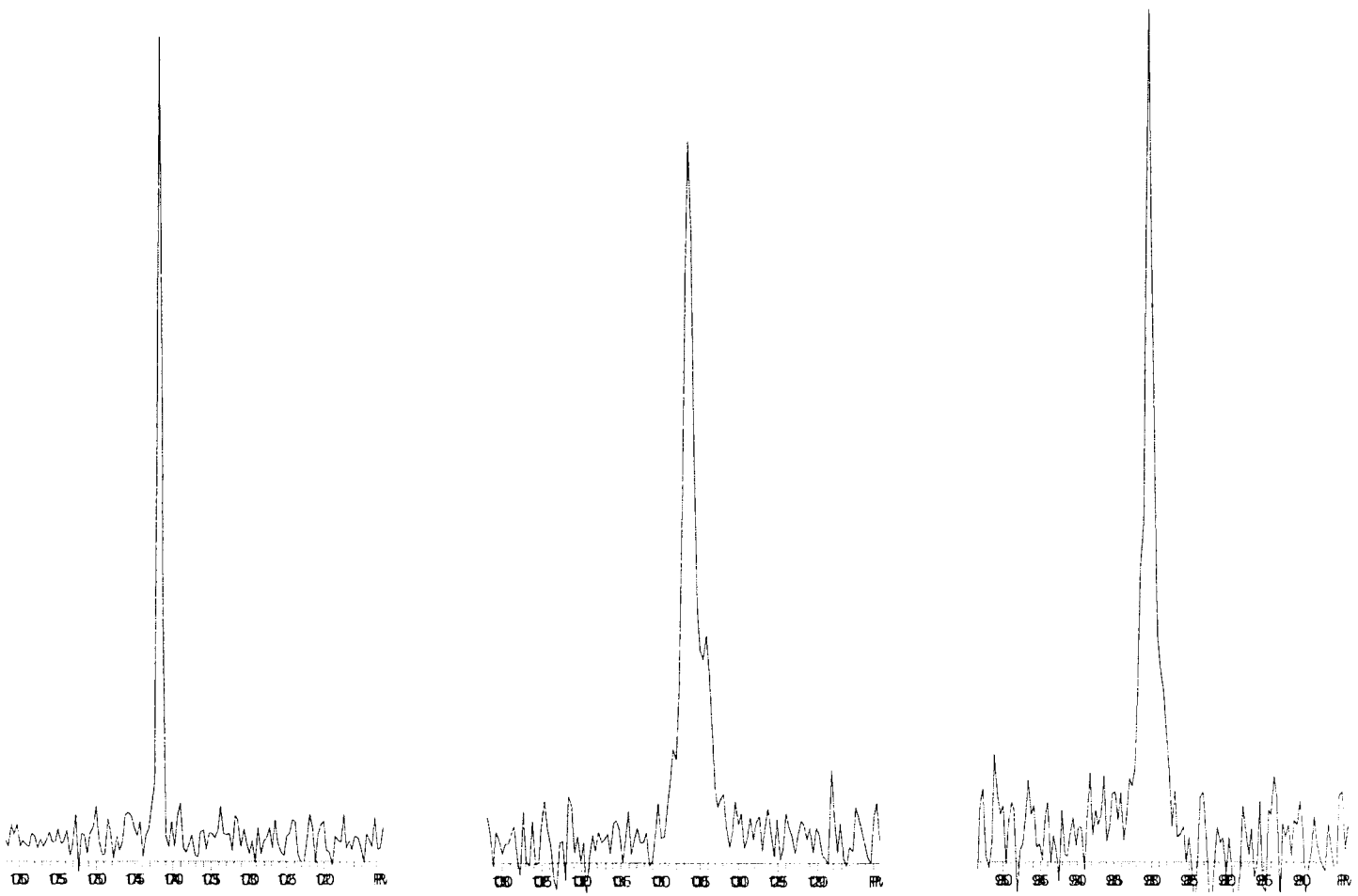

Line shape reference
107.1 (Tp' Vinyl)

102.8

98.0

Figure 2.17: Spectra of Unlabeled Tp'Re(O)*trans*-1,2-cyclooctanediolate

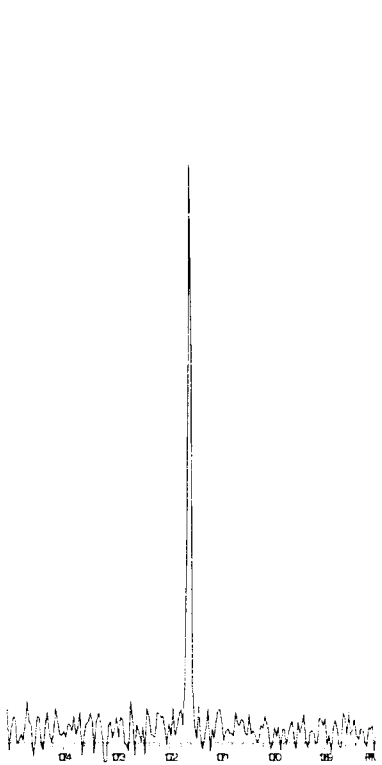

Line shape reference
107.1 (Tp' Vinyl)

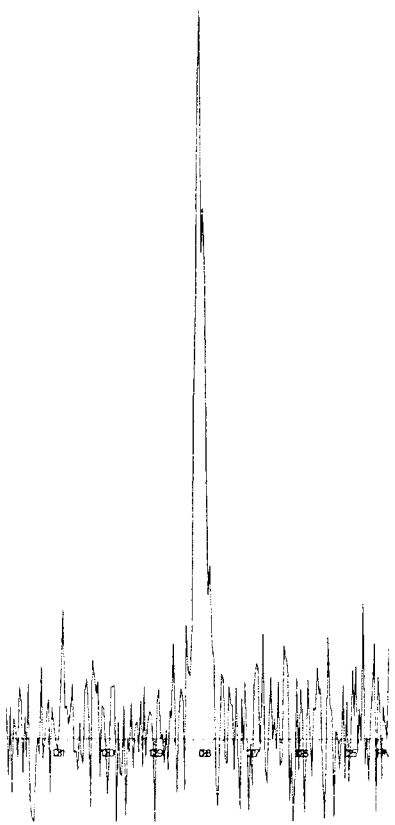

102.8

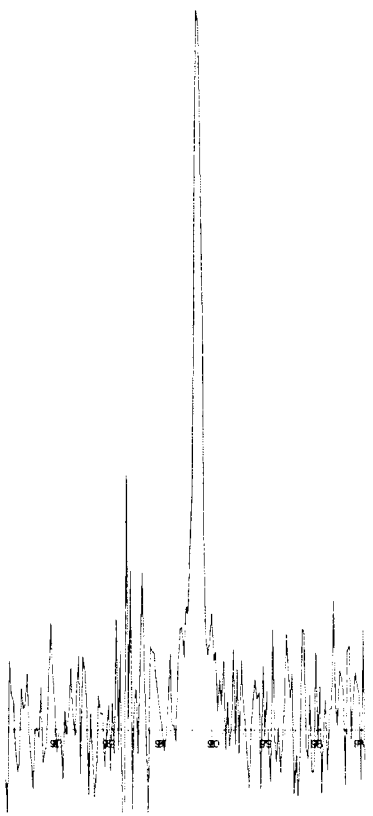

98.0

Synthesis of a Rhenium Dimer Complex

One of the attempted syntheses of Tp'$ReOCl_2$ led to the synthesis of an interesting dimeric compound reported in 1987 by Enemarck and Backes-Dahmann.[49] The procedure used by Mayer[50] in his synthesis of $TpReOCl_2$ was used in this attempt to make the analogous Tp' compound (see Figure 2.18). To a solution of $KReO_4$ in ethanol, aqueous HCl was slowly added, and then KTp' was added. The mixture was heated to reflux for 2 hours. Prior to heating, the solution had only a slight hint of yellowish coloring, and some white KTp' did not dissolve. After 15 minutes of heating, the solution turned a deeper yellow color, with some KTp' still not in solution. When the heat was removed, the mixture slowly turned blue-green over 15 hours at room temperature. When the green solution was heated up again, it turned yellow again, then turned green again at room temperature. The mixture was purified by filtering to remove undissolved KTp', and chromatography on silica using methylene chloride to elute. Light also seems to help this reaction–if the reaction flask is covered after removal from heat, the mixture turns green more slowly than if exposed to light. Later, the purified green compound was dissolved in ethanol and heated--this did not turn yellow. It is clear that the other reactants are needed to break down the green compound.

Characterization of the Rhenium Dimer Complex

The x-ray crystal structure quickly showed that this green compound was not the desired Tp'$ReOCl_2$. The structure showed that it was a dimer complex with the two rhenium atoms joined by a bridging oxo (Figure 2.19). It is interesting that the two 3,5-dimethylpyrazole (Pz) rings on each rhenium are *cis* to each other. This is not at all what would be expected based on steric arguments.

The IR spectrum of this compound also showed that it was not Tp'$ReOCl_2$. A few features of the IR spectrum that are worth noting are the N-H stretch, which is a strong, broad signal at 3222 cm^{-1}, the signal at 971 cm^{-1}, which is probably the rhenium-oxo stretch, and the lack of any signals in the 2500-2700 cm^{-1} range, which shows that there is no B-H stretch.

Figure 2.18: Synthesis of Rhenium Dimer Complex

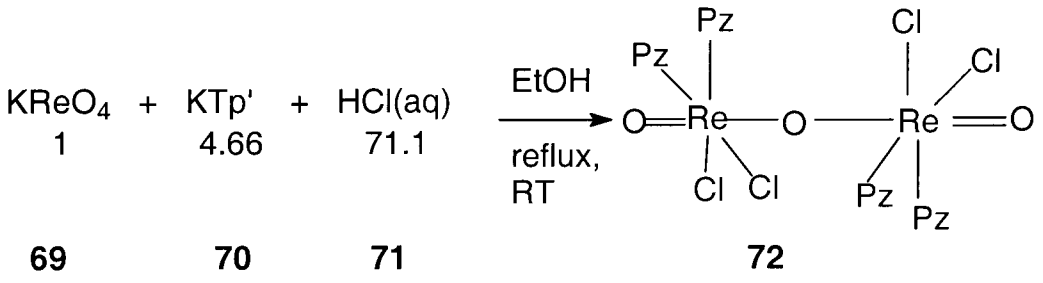

Figure 2.19: X-ray Crystal Structure of Rhenium Dimer Complex

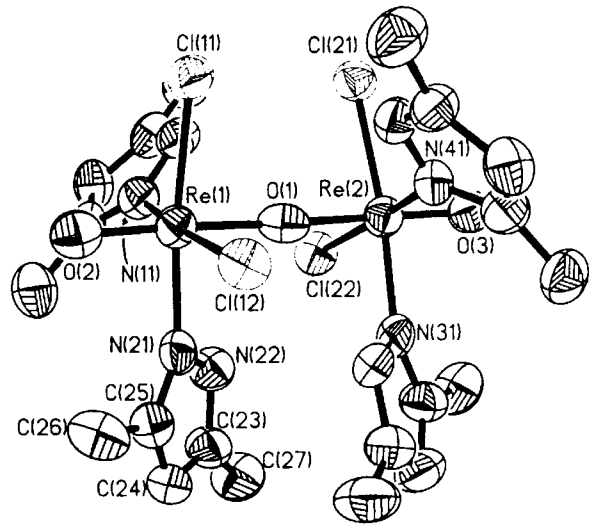

The low resolution mass spectrum of this dimeric species was consistent with the x-ray structure. The spectrum contains peaks at 850 m/z which are similar to the calculated pattern for the molecule less one pyrazole ring. The peaks at 779 m/z match the pattern calculated on the Sheffield Chemputer for the molecule less one pyrazole ring and two chlorines. In like manner, the peaks centered around 719 m/z fit the molecule less two pyrazole rings and one chlorine. The fragments calculated to fit the peaks and peak value with the largest intensity of the group of peaks in m/z are shown in Table 2.2.

The variable temperature ^{1}H NMR data also make sense in light of the crystal structure. In Figure 2.20, the room temperature ^{1}H NMR spectrum of this compound shows broad peaks. However, since the peaks become narrow at 265 K, the broad peaks

Table 2.2: Mass to Charge Ratios and Formulas of Corresponding Fragments

Large peak (m/z)	Formula of fragment
850	$C_{15}H_{24}Cl_4N_6O_3Re_2$
779	$C_{15}H_{24}Cl_2N_6O_3Re_2$
719	$C_{10}H_{16}Cl_3N_4O_3Re_2$
465	$C_{10}H_{16}Cl_2N_4ORe$
446	$C_{10}H_{16}Cl_2N_4Re$

at room temperature are a function of some sort of dynamic process that slows down at lower temperatures, not a result of paramagnetism. Furthermore, when the ^1H NMR experiments were done above room temperature, some of the peaks coalesced with each other. For example, the peaks at 10.8 and 11.6 ppm coalesce at 318 K, and the peaks at 5.9 and 6.0 coalesce at 303 K (Figure 2.20). (In Figure 2.20, peaks marked with "X" are impurities in the $CHBr_3$, which was used as the solvent at 330 K and 360 K; $CDCl_3$ was used for temperatures between 265 K and 318 K.) From these four sets of peaks which coalesce at different temperatures, the activation parameters can be calculated (Table 2.3). The rate constant for the coalescence temperature can be found[51] using the equation $k = (\pi\Delta\nu)/(\sqrt{2})$, where k = rate constant at the coalescence temperature, $\Delta\nu$ = distance in hertz between the initially sharp lines. The $\Delta G^{\ddagger}$ for this process can be found by using this equation: $\Delta G^{\ddagger} = RT_c[23 + \ln(T_c/\Delta\nu)]$, where $\Delta G^{\ddagger}$ = free energy of activation, R = gas constant, T_c = coalescence temperature, $\Delta\nu$ = distance in hertz between the initially sharp lines. The free energy of activation for all four is within 15 $\pm$ 0.1 kcal/mol, which is consistent with the same process causing all of the exchange.

The entropy of activation is also close to zero–which indicates an intramolecular process. This process is probably rotation about the Re-(μ-O)-Re link.

Figure 2.20: Variable Temperature NMR Spectra of Rhenium Dimer Complex

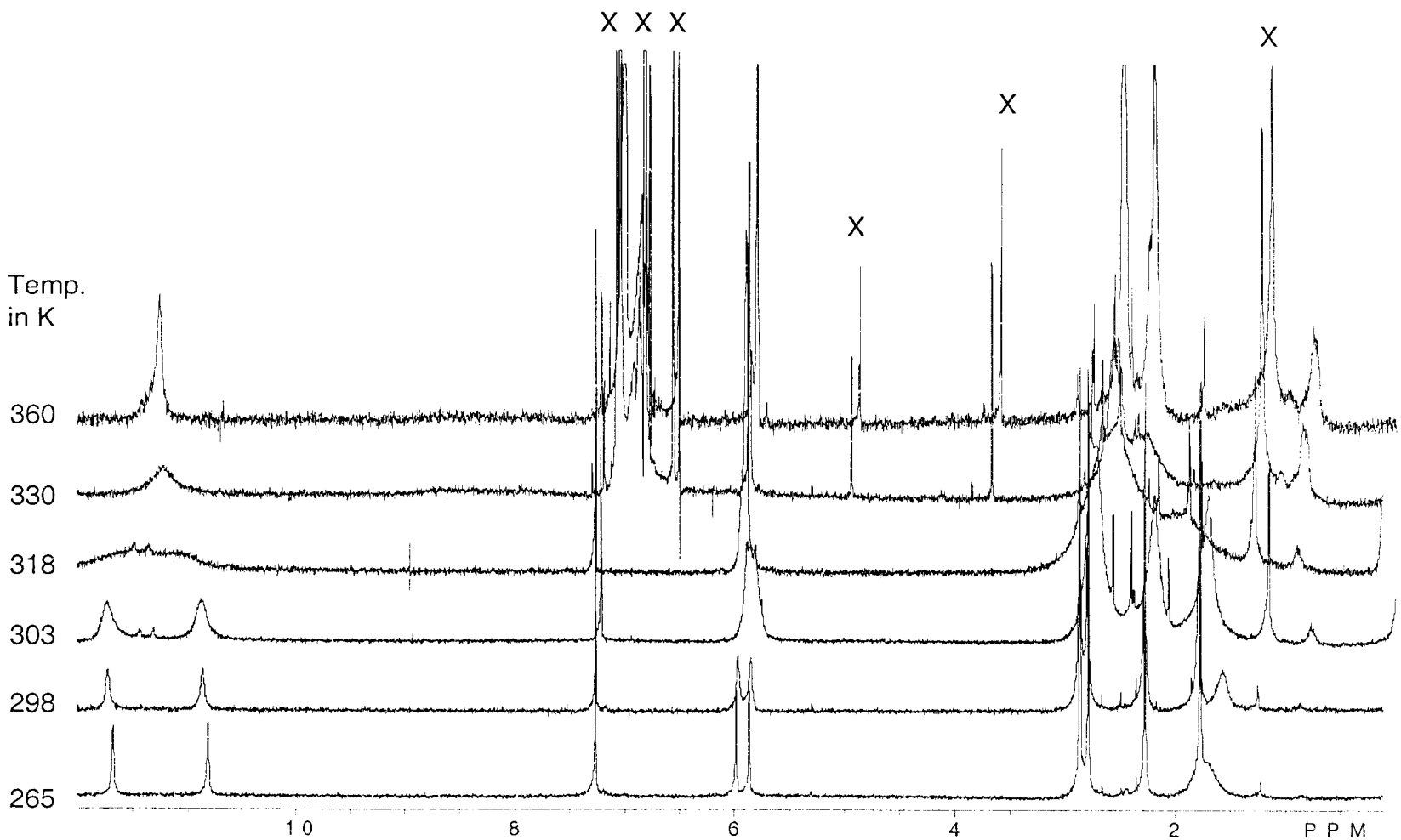

Table 2.3: Activation Parameters

NMR Coalescence and Rate Data for Compound **72**

δ, Low-T Limit	Δν, Hz	T_c, K	k at T_c, s^{-1}	$\Delta G^{\ddagger}$, kcal/mol
11.67, 10.81	345	330	767	15.0
5.99, 5.86	49	306	109	15.1
2.86, 2.26	237	325	527	15.0
2.79, 1.77	406	333	902	15.1

$\Delta H^{\ddagger} = 15.5 \pm 0.7$ kcal/mol

$\Delta S^{\ddagger} = 1.8 \pm 6.7$ cal/(mol-K)

δ, Low-T Limit = Distinct signals at low temperature which merge at high temperatures.

Δν, Hz = Separation in Hertz of the signals at low temperature.

T_c, K = Coalescence temperature in Kelvin.

k at T_c = rate constant at the coalescence temperature, calculated from $k = \pi\Delta\nu/(\sqrt{2})$

$\Delta G^{\ddagger}$ = Free enengy of activation, calculated from $\Delta G^{\neq} = RT_c[23 + 2.3 \log (T_c/\Delta\nu)]$ KJ/mol

$\Delta H^{\ddagger}$ = Enthalpy of activation

$\Delta S^{\ddagger}$ = Entropy of activation, $\Delta H^{\ddagger}$ and $\Delta S^{\ddagger}$ calculated from $\Delta G^{\ddagger} = \Delta H^{\ddagger} - T\,\Delta S^{\ddagger}$

Chapter 3. Conclusions

The experiments using *tris*-(3,5-dimethylpyrazolyl)-hydridoborato rhenium (oxo) *trans*-1,2-cyclooctanediolate have shown that one C-O bond breaks faster than the other. This is another indication that the cycloreversion of rhenium diolates occurs by a stepwise process. It may also indicate that the osmium tetraoxide oxidation of olefins occurs via a stepwise process, for cycloreversion is the microscopic reverse of this reaction. This experiment also does not demonstrate the presence of a metallaoxetane; all it demonstrates is that one C-O bond breaks faster than the other. Although it is unlikely, this could be caused by a very "asynchronous concerted" transition state. It is also possible that an intermediate other than the metallaoxetane is formed during the stepwise process. For example, coordinated epoxide has also been proposed[52] as the intermediate in a stepwise process (see Figure 3.1). Caution may also be warranted in applying the results from the rhenium system to the osmium system.

Figure 3.1: Alternative Stepwise Mechanism Involving Epoxide Intermediate

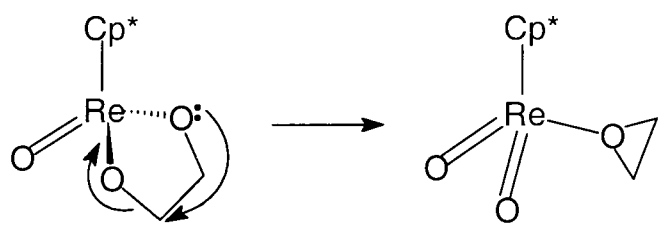

73 **74**

Chapter 4. Experimental

General Techniques

Methods used in working with air-sensitive compounds are described in the literature.[53] Unless otherwise noted, chemicals were used as received from Aldrich. Solvents were distilled prior to use from potassium or calcium hydride, or in the case of THF, sodium/benzophenone. DMSO was purified by vacuum distillation from calcium hydride. The field strengths of the Bruker AC300 and AM400 NMR spectrometers used were 300.13 MHz and 400.13 MHz, respectively. (The AC300 instrument was usually used for ^{1}H NMR, and the AM400 instrument was used for ^{13}C NMR , COSY, HETCOR, and NOE.) The IR instrument used was a Nicolet Magna-IR 560 spectrometer.

Synthesis of Tp'ReO_3

Tp'ReO_3 was made according to Herrmann's procedure.[54] To a 50 mL round bottom flask with a stir bar was added 1.1369 g (2.34 mmol) of Re_2O_7 and 0.836 g (2.49 mmol) of KTp'. Dry THF (20 mL) was vacuum transferred to the flask. The mixture was allowed to stir at RT under argon for 1 hour. The white trioxide was then filtered and washed with hot water and acetone. The mass of Tp'ReO_3 that was isolated was 0.4988 g (1.87 mmol), and the percent yield was 39.9%. IR (KBr pellet): 3432(w), 3145(w), 2930(w), 2547(w), 2361(w), 1545(s), 1452(s), 1417, 1389, 1372(s), 1214(s), 1190,

1070(s), 1049(w), 991(w), 938, 909(s), 866(w), 815(w), 787(w), 688(w), 647(w), 478(w), cm^{-1}. Coe[55] reports: 2550(m), 2540 (w), 940(m), 920(s), 910(s), cm^{-1}.

Ring-opening of Cyclooctene Oxide

Conditions for converting Z-cyclooctene oxide to *trans*-1,2-cyclooctanediol were examined by preparing solutions of epoxide in 0.5 mL of solvent and adding the solutions to NMR tubes. (The NMR tubes for the first two entries were sealed under vacuum.) The different conditions used are shown in Table 4.1.

Table 4.1: Reaction Conditions for NMR Tube Scale Syntheses of Cyclooctanediol

cyclooctene oxide(mg)	reagent/ concentration	temperature (°C)	time	result
5.5	KOH/1.08M	122	8 days	no reaction
6.6	H_2SO_4/0.81M	RT	11 hrs	rxn complete
6.0	H_2SO_4/0.01M	RT/35	72hrs/6 days	rxn complete
6.8	H_2SO_4/0.78M	35	48 hrs	rxn complete

In most cases, the amount of liquid in the reaction was 0.5 ml, and the solvents used were 75% DMSO-d_6 and 25% D_2O. (The exception is the second entry, where the percent of D_2O is 16.4%.) Based on these results, the scale-up of this reaction was done by adding 486 mg of cyclooctene oxide to a 1 N solution of sulfuric acid in water/DMSO (2.6mL/9.5mL) and heating in an oil bath for 5 days. The mixture was then extracted with 6 mL of chloroform four times. The chloroform was then extracted three times with 6 mL saturated aqueous NaCl to remove DMSO. The chloroform was

dried over $MgSO_4$, and solvent was reduced by rotary evaporation. The mixture was then purified by column chromatography on silica gel using a 36 cm length of silica gel in a 1 cm radius column with ethyl acetate to elute. The fractions which contained the cyclooctanediol were then combined and solvent stripped off. The resulting mixture still had ethyl acetate in it, but the *trans*-1,2-cyclooctanediol was as pure as commercial material apart from that. (The ^1H NMR spectrum of the commercially available *trans*-1,2-cyclooctanediol was very similar to the spectrum of the compound obtained.)

Synthesis of the ^{18}O labeled *trans*-1,2-cyclooctanediol

To a 50 mL round bottom flask was added 7.30 mL of DMSO (freshly distilled from calcium hydride), 0.305 mL of concentrated aqueous H_2SO_4, 2.0 mL of $H_2{}^{18}O$ (ordered from Icon,96 atom-%^{18}O), and about 677.5 mg of Z-cyclooctene oxide, in the order listed. The reaction flask was sealed with a greased stopcock and allowed to stir in an oil bath which was 28 °C on the first day, 31 °C on the second day, 36 °C on the third day, 41 °C on the fourth and fifth days. On the fifth day, the reaction mixture was removed from heat and extracted four times with 5 mL of chloroform. The chloroform was then extracted three times with 5 mL of aqueous NaCl solution. The chloroform was then dried over $MgSO_4$, and the solvent reduced by rotary evaporation. Column chromatography was then used to purify the diol. The silica used was Selecto Scientific brand with particle size 32-63 and lot number of 22521. The column was 1 cm in radius and had 1.5-2 cm of glass wool at the bottom, followed by 1 cm of sand, followed by 20 cm of silica. Ethyl acetate was used to make the column and to elute the diol. Fifteen

fractions each containing about 15 mL were collected. The *trans*-1,2-cyclooctanediol was detected in fractions 5-10, although 5 and 6 appeared to have some impurity in the diol according to the TLC. This impurity was not significant enough to show up in the ^{1}H NMR. Total diol yield is 582.6 mg, which is about 83 % yield. The diol had small amounts of ethyl acetate in it, so it was a viscous, clear liquid. However, about a week in a desiccator caused the diol to crystallize. Characterization: ^{1}H NMR: 1.51, 1.64, and 1.82 (br m, 12 H, not resolved), 2.88(s, 2 H), 3.56(br s, 2 H), 7.27($CDCl_3$). ^{13}CNMR: 23.6, 26.1, 31.9, 76.1, center peak of $CDCl_3$ triplet at 77.0 ppm.

Synthesis of Tp'rhenium(oxo)*trans*-1,2-cyclooctanediolate

This was done as previously reported.[56] To a 50 mL round bottom flask equipped with a stir bar was added 167.3 mg (0.309 mmol) of Tp'ReO_3 , 470 mg (3.26 mmol) of *trans*-1,2-cyclooctanediol, 112.0 mg of PPh_3 (polymer supported, 3 mmol P/g resin), 69.0 mg (3.62 mmol) of p-toluenesulfonic acid monohydrate, and 1.21 gram of dried, crushed 4 Å molecular sieves, and the flask then was attached to a double ended frit tube. Dry THF (20 mL) was vacuum transferred to the flask, and the mixture was allowed to stir at RT under argon for 15 hours. The mixture changed from beige to bluish beige. The blue solution was filtered off of the brown polymer/molecular sieve mixture and the solvent stripped off. The blue diolate was then recrystallized from ethanol/water and rinsed with hexane to remove grease; 111.4 mg was obtained at a 55.5% yield. Tp'Re(O)*trans*-1,2-cyclooctanediolate was characterized by IR, ^{1}H NMR, ^{13}C NMR, COSY, HETCOR, NOE experiments, and low resolution mass spectroscopy.

IR (solution cell,CH_2Cl_2): 3949.89, 3756.89, 3692.92, 3053.97, 2986.33, 2926.51, 2854.17, 2685.57, 2546.91, 2410.45, 2305.62, 2126.77, 2054.46, 1721.96, 1602.16, 1543.66, 1452.40, 1421.71, 1384.27, 1264.87, 1203.99, 1072.69, 947.70, 895.98, 739.26, cm^{-1}

NMR results are summarized in Table 4.2.

Table 4.2: NMR Results from 2D COSY and HETCOR Experiments

HNMR shifts,ppm	Coupled protons	Coupled carbon(s)
1.88 (3 H)		11.80 or 11.94
2.45 (3 H)		14.86
2.19 (3 H)		11.80 or 11.94
2.76 (3 H)		13.98
2.82 (3 H)		13.52
2.51 (3 H)		14.86
5.66 (2 H)		107.2
5.66 (2 H)		107.3
5.22 (1 H)		106.4
5.68 (1 H)	4.97,1.83,2.41	97.63
4.97 (1 H)	5.68,2.63,2.98	102.2
1.83(1 H),2.41(1 H)	5.68,1.47,1.74	38.11
2.63(1 H),2.98(1 H)	4.97,1.70,1.99	37.53
1.47(1 H),1.74(1 H)	1.83,2.41	28.20
1.70(1 H),1.99(1 H)	2.63,2.98	24.38
1.39(1 H),1.71(1 H)	?	27.39
1.60 (2 H)	?	22.98

Table 4.3 is a summary of the results of searching for a good solvent that would neither broaden the signals at 102 ppm and 97 ppm nor give a small signal to noise ratio. (The last entry is from a DEPT spectrum, whereas the others are from ordinary ^{13}C NMR spectra.)

Table 4.3: Other NMR Data for Tp'Re(O)*trans*-1,2-cyclooctanediolate

Solvent	Line width, 103 ppm	Line width, 98 ppm	Signal-to-Noise Ratio
acetone-d6	2.8 Hz	1.9 Hz	3.00
benzene-d6	3.2 Hz	2.4 Hz	4.76
$CDCl_3$	4.4 Hz	3.5 Hz	7.00
4:1 acetone:$CDCl_3$	1.9 Hz	2.4 Hz	13.3

Synthesis of Oxygen-18 Labeled Tp'rhenium(oxo)*trans*-1,2-cyclooctanediolate

The procedure used to make the labeled diolate was the same as the procedure used to make the unlabeled compound, except that labeled *trans*-1,2-cyclooctanediol was used, only 0.2 eq. of p-toluenesulfonic acid was used, and the PPh_3 used was not polymer supported. To a 50 mL round bottom flask equipped with a stir bar 408.9 mg(0.772 mmol) of Tp'ReO_3, 29.2 mg (0.154 mmol) of p-toluenesulfonic acid, 321.8 mg (2.23 mmol) of oxygen-18 labeled *trans*-1,2-cyclooctanediol (about 19% oxygen-18 labeled), 625.3 mg (2.38 mmol) of PPh_3, and about 1.2 g of dried molecular sieves were added. This flask was then attached to a double ended frit tube, and 25 mL of THF was vacuum transferred to it. The reaction mixture was stirred at room temperature for 16

3/4 hours and then filtered. The reaction mixture began as a beige suspension and changed to an intense blue color. After the THF was stripped off, the mixture was purified by column chromatography. A 1 cm column was packed with 2 cm of glass wool, 1.5 cm of sand, and 21 cm of silica gel in chloroform. The blue diolate was eluted from the column slowly with chloroform; eventually 540 mL of chloroform containing diolate was eluted. The solvent was stripped off of this immediately by rotary evaporation. Some faint blue colored stuff did not move from the bottom of the column until application of a 3:2 chloroform/ethyl acetate mixture, but when this came off, it was greenish in color. Twenty 15 mL fractions of ethyl acetate were also eluted from the column to recover the excess diol, which was found to be in fractions 12-17 by TLC. After chromatography, the yield of Tp' rhenium(oxo) *trans*-1,2-cyclooctanediolate was 244.9 mg, or 49.6%. This diolate was characterized by DEPT NMR (with toluene-d8 as solvent and AM 400 spectrometer). The DEPT NMR was identical to the spectrum of the unlabeled compound, except for the shoulders on the peaks at 98 and 103 ppm, which could be seen in 4:1 acetone-d6/$CDCl_3$. The low resolution mass spectrum of the labeled compound was compared with the mass spectrum of the unlabeled compound; Table 4.4 shows the intensities of the peaks around 640 m/z, which is the molecular weight.

Kinetics Experiments on the Tp'Re(O)*trans*-1,2-cyclooctanediolate

A solution of diolate in toluene-d8 was added to seven NMR tubes which were then sealed under vacuum and stored in a freezer. A constant temperature oil bath was heated

up to 106.3 °C, and the NMR tubes were heated in the bath for 0.5 hr., 1 hr., 2 hrs.,5 hrs., 10 hrs., 30 hrs., and 72 hrs. After heating, the tubes were immediately stored in the freezer. They were then cracked open, the toluene stripped off of each one separately on the vacuum line, and the dry diolate redissolved in a 4:1 mixture of acetone-d6 and chloroform-d so that the diolate solution could be sealed into NMR tubes. The NMR experiments were performed using the Bruker 400 NMR instrument which is 100 MHz for carbon spectra.

Table 4.4: Mass Spectrum Peak Intensities for Labeled and Unlabeled Diolates

Mass	Intensity for Unlabeled	Intensity for Labeled
636	0.35	0.8
637	0.29	0
638	0.76	1.67
639	4.06	8.36
640	14.63	18.97
641	11.98	15.01
642	25.79	32.66
643	9.47	9.29
644	7.36	2.38
645	2.34	0
646	0.34	0
648	0.27	0
649	0	2.02
650	0	3.6

The temperature was regulated by passing air through tubing that was cooled off by ice into the instrument and by using a setting of the heater on the instrument so that the temperature as read on the instrument stayed at 298 K.

Tetrachloro-μ-oxodioxotetrakis-3,5-dimethylpyrazoledirhenium (V)

To a 50 mL round bottom flask with a stir bar was added 101.8 mg (0.352 mmol) of $KReO_4$, 561mg (1.64 mmol) of KTp', 1.67 mL of concentrated aqueous HCl and 20 mL of ethanol. The mixture was heated to reflux for about 8 hours in the air and allowed to stand at RT with no heat but with stirring for 18 hours, at which point stirring was turned off for 7 hours and resumed for 5 days. At the end of the reflux time, the mixture was yellow; but after 12-15 hours at RT the mixture was bright green. The green material was isolated by column chromatography on silica gel using dichloromethane. The column had a diameter of 1 cm and a height of 55 cm. The column contained 3 cm of glass wool, 2 cm of sand, and 50 cm of silica gel (Selecto Scientific, lot #22521, particle size 32-63) under dichloromethane. The sample was eluted with 200 mL of dichloromethane, and the solvent was stripped using rotary evaporation. The mass of product obtained was 0.0891 g (0.0946 mmol), for a 53.74% yield. The tetrachloro-μ-oxodioxotetrakis-3,5-dimethylpyrazoledirhenium (V) was characterized by IR, low resolution mass spectroscopy, ^1H NMR at different temperatures, and x-ray crystallotography.

IR (KBr pellet): 3222(s), 3145, 3041, 2975, 2927, 2362(w),1610(w),1577(s), 1477, 1408(s), 1375, 1280, 1180,1153(w),1060, 1029, 970, 812, 753(s), 688(w),656, 613,443. Reported values[57] are 3223(vs), 3146(sh), 972(s), 704(s,br). The mass spectrum showed the following centers of clusters of peaks: 850, 779, 719, 465, 446, 429, 369, 350, 333, 307. The variable temperature ^1H NMR spectra were obtained on a Bruker am 400 instrument. About 10 mg of the compound was dissolved in about 0.5 ml of $CDCl_3$.

The temperature was calibrated by measuring the $\Delta\delta$ of the two signals in 80% ethylene glycol/DMSO-d6 at each different temperature. ^{1}H NMR signals at 275 K in ppm: 1.8 (6 H), 2.3(6 H),2.85 and 2.9 (not resolved, 12 H),5.9 (2 H),6.0 (2 H),10.8 (2 H),11.6 (2 H). ^{1}H NMR signals at 303 K in ppm: 1.8 (6 H),2.3 (6 H),2.8 (12 H),5.95 (4 H),10.8 (2 H),11.6 (2 H). Other temperature changes in spectra can be seen in Figure 2.20. Room temperature ^{1}H NMR signals reported[58] in the literature: 2.27, 2.32(s), 5.86(s), 6.13(s), 10.9(br, w).

X-ray Structure of Tetrachloro-μ-oxodioxotetrakis-3,5-dimethylpyrazoledirhenium (V)

The x-ray crystal structure analysis was done on a large, singe crystal mounted on the end of a Pyrex fiber using epoxy glue. The radiation was from copper, and the wavelength was 1.54178 Å. Lattice parameters were determined by an automated search that yielded the setting angles of 56 peaks with $10.5<2\theta<70.0$. Data collection was performed as described elsewhere.[59] The data were corrected for the effects of decay (25%) by a linear interpretation of the standards, and for the effects of absorption anisotropy by an analytical procedure based on face indexing.

The space group ($P2_1$, #4) was determined by careful examination of the only systematic extinction present in the data, {(0,k,0), k = 2n + 1}, and confirmed by successful solution and refinement of the structure in this space group. While there are four serious violations of the systematic absence condition, the value of the reflections of this class has an average I/σ of ca. 6, compared to an average value of 30 for all other

reflection classes. The intensity measured for these reflections is therefore likely due to double reflection (also known as the Renniger effect).[60]

A solution was obtained by Patterson map interpretation as programmed in SHELXS-90[61] and this solution was extended by successive cycles of least squares refinement followed by Fourier synthesis using the program SHELXL-93.[62] During the final cycles, all non-hydrogen atoms were refined using anisotropic displacement parameters. Hydrogen atoms were placed in geometrically calculated positions on the carbon on the 4 position of the pyrazole rings, and on the unbound nitrogen, and given common isotropic thermal displacement parameters. All methyl group hydrogen atoms were placed in idealized positions and given a displacement parameter equal to 1.2 times that of the carbon to which they are attached. Some large peaks remain in the final electron density map (up to 1.5 $e^-/Å$), but they are all very close to the rhenium atoms and are not of chemical significance.

While the space group in which the molecule crystallized is acentric, refinement of the Flack parameter,[63] which converged to a value of 0.43(5), shows that the crystal must contain a racemic mixture of the enantiomers of the molecule seen in the crystal structure. Crystallographic data may be found in the Appendix.

Endnotes

1.Ittel, S.D.; Parshall, G.W. *Homogeneous Catalysis*, 2nd Ed.; John Wiley & Sons: New York, 1992, 150.

2.ibid., 154.

3.Palucki, M.; McCormick, G.J.; Jacobsen, E.N. *Tetrahedron Letters* **1995**, *36*, 5457-5460.

4.Shilov, A.E.; Shul'pin, G.B. *Chem. Rev.* **1997** , *97*, 2679-2932.

5.a) Periana, R.A.; Taube, D.J. *Science* **1993**, *259*, 340-343.
b) Periana, R.A.; Taube, D.J. *Science* **1998**, *280*, 560-564.

6.Ittel, S.D.; Parshall, G.W. *Homogeneous Catalysis*, 2nd Ed.; John Wiley & Sons: New York, 1992, 156.

7. Hoeldrich, W.F. In *Heterogeneous Catalysis and Fine Chemicals*; M. Guisnet, Ed. Elsevier Science Publishers: Amsterdam, 1988, 83.

8.Albert, H.J. In *Mcgraw-Hill Encyclopedia of Science and Technology*, 6th Ed., S. P. Parker, Ed.,Volume 12; McGraw-Hill: New York,1987, 562.

9.Ittel, S.D.; Parshall, G.W. *Homogeneous Catalysis*, 2nd Ed.; John Wiley & Sons: New York, 1992, 157.

10.Norrby, P.-O. ; Gable, K. P. *J. Chem. Soc., Perkin Trans. 2* **1995** , 171-178.

11.Criegee, R. *Justus Liebigs Ann. Chem.* **1936**, *522*, 75-96.

12.Corey, E.J.; M.C. Noe, and S. Sharsan *J. Am. Chem. Soc.* **1993**,*115*, 3828-3829.

13.Sharpless, K.B. *J. Am. Chem. Soc.* **1977**, 3120

14.Nugent, W.A.; Mayer, J.M. *Metal-Ligand Multiple Bonds*, John Wiley & Sons: New York, 1988, 256.

15.Gable, K.P. *Adv. Organomet. Chem.* **1997**, vol. 41, 127-161.

16.(a)Herrmann, W.A.;Kuchler, J.G.;Weichselbaumer, G.;Herdtweck, E.; Kiprof, P.J. *Organomet. Chem.* **1989**, *372*, 351-370.
(b) Herrmann, W.A.;Kuhn, F. E.;Rauch, M.U.;Correia, J.D.G.;Artus, G. *Inorg. Chem.* **1995**, *34*,2914-2920.

17.ref. 12

18.Torrent, M.; Deng, L.; Duran, M.; Sola, M.; Ziegler, T. *Organometallics* **1997**, *16*, 13-19.

19.DelMonte, A. J.; Haller, J. ; Houk, K. N.; Sharpless, K. B.; Singleton, D. A. ; Strassner, T.; Thomas, A. A. *J. Am. Chem. Soc.* **1997**, *119*, 9907-9908.

20.(a)Veldkamp, A.;Frenking, G. *J. Am. Chem. Soc:* **1994**, *116*,4937.
(b)Norrby,P.-O.;Kolb, H.C.; Sharpless, K.B. *Organometallics* **1994**, *13*, 344.

21.Gobel, T. and Sharpless, K.B. *Angew. Chem. Int. Ed. Engl.* **1993**, *32*, no. 9, 1329.

22.Gable, K.P.;Phan, T.N. *J. Am. Chem. Soc.* **1994**, *116*, 833-839.

23.Herrmann, W. A.;Marz, D.W.;Herdtwick, E.;Schafer, A.;Wagner, W.;Kneuper, H.-J. *Angew. Chem. Int. Ed. Engl.* **1987**, *26*, 462-464.

24.Gable, K.P. *Organometallics* **1994**, *13*, 2486-2488.

25. a) Paulo, A.; Domingos, A.; Marcalo, J.; Pires de Matos, A.; Santos, I. *Inorg. Chem.* **1995**, *34*, 2113-2120.
b) Gable, K.P.;AbuBaker, A.;Zientara, K.;Wainwright, A.M. *Organometallics* **1999**, *18*,173-179.

26.Carey, F.A. and R. J. Sundberg *Advanced Organic Chemistry*, 3rd Ed., Part A; Plenum: New York, 1990, 193.

27.Herrmann, W. A.;Marz, D.; Herdtwick, E;Schafer, A; Wagner, W.; Kneuper, H.-J. *Angew. Chem., Int. Ed. Engl.* **1987**,*26*, 462-464.

28.Gable, K.P.;AbuBaker, A.;Zientara, K.;Wainwright, A.M. *Organometallics* **1999**, *18*,173-179.

29.Gable,K.P.;Phan,T.N. *J. Am. Chem. Soc.* **1994**, *116*, 833-839.

30.ibid.

31.Gable, K.P.; Phan, T. N. *J. Am. Chem. Soc.* **1993**, *115*, 3036-3037.

32.Gable, K.P.; Phan, T.N. *J. Am. Chem. Soc.* **1994**, *116*, 833-839.

33.Carey, F.A. and R. J. Sundberg *Advanced Organic Chemistry*, 3rd Ed., Part A; Plenum: New York, 1990, 211-215.

34.Gable, K.P.;Juliette, J.J.J. *J. Am. Chem. Soc.* **1996**, *118*, 2625-2633.

35.Carey, F.A. and R. J. Sundberg *Advanced Organic Chemistry*, 3rd Ed., Part A; Plenum: New York, 1990, pp. 196-207.

36.Carey, F. A and R. J. Sundberg *Advanced Organic Chemistry*, 3rd Ed., Part A; Plenum: New York, 1990, 207-208.

37.Gable, K.P.;Juliette, J.J.J. *J. Am. Chem. Soc.* **1996**, *118*, 2625-2633.

38.Gable, K.P.;Juliette, J.J.J. *J. Am. Chem. Soc.* **1995**, *117*, 955-962.

39.Frenking, G.; Deubel, D.V. *J. Am. Chem. Soc.* **1999**, *121*, 2021-2031.

40.ref. 23.

41.Carey, F.A. and R. J. Sundberg *Advanced Organic Chemistry*, 3rd Ed., Part A; Plenum: New York, 1990, 193.

42.Gable, K.P. *Organometallics* **1994**, *13*, 2486-2488.

43.Paulo, A.; Domingos, A.; Marcalo, J.; Pires de Matos, A.; Santos, I. *Inorg. Chem.* **1995**, *34*, 2113-2120.

44.Coe, B.J. *Polyhedron* **1992**, *11*, no. 9, 1085-1091.

45.Enemarck, J. H.; Backes-Dahmann, G. *Inorganic Chem.* **1987**, *26*, 3960-3962.

46.Berti, G.; Macchia, B.; Macchia, F. *Tetrahedron Letters* **1965**, *38*, 3421-3427.

47.Denmark, S.E.;Barsanti, P.A.;Wong, K.-T.; Stavanger,R.A. *J. Org. Chem.*, **1998**,*63*, 2428-2429.

48.Sheffield ChemPuter online, www.shef.ac.uk/~chem/chemputer/isotopes.html

49.Enemarck, J. H.; Backes-Dahmann, G. *Inorganic Chem.* **1987**, *26*, 3960-3962.

50.Mayer, J. and S. Brown. *Inorganic Chem.* **1992**, *32*, 4091.

51.Williams, D.H.; Fleming, I. *Spectroscopic Methods in Organic Chemistry*, 5th Ed.; McGraw-Hill: London, 1995, 104-105.

52.Gable, K.P.; Juliette, J.J.J. *J. Am. Chem. Soc.* **1996**, *118*, 2625-2633.

53.Shriver, D. F. and M. A. Drezdzon. *Manipulation of Air-sensitive Compounds.* Wiley: New York, 1986.

54.Herrmann, W. A. *Chem. Ber.*, **1990**, *123*, p. 1347.

55.Coe, B.J. *Polyhedron* **1992**, *11*, no. 9, 1085-1091.

56. (a)Gable, K. P. *Organometallics*, **1994**, *13*, 2486-2488.
(b)Gable, K. P.; AbuBaker, A.; Zientara, K.; Wainwright, A. *Organometallics* **1999**, *18*, 173-179.

57.Enemarck, J. H.; Backes-Dahmann, G. *Inorganic Chem.* **1987**, *26*, 3960-3962.

58.ibid.

59.Alex Yokochi, personal communication.

60.Dunitz, J. D. *X-Ray Analysis and the Structure of Organic Molecules*, 2nd Corrected Reprint; VCH publishers, Inc.: New York, 1995.

61.Sheldrick, G.M. *Acta Crystallogr.* **1990**, *A46*, 467.

62.Sheldrick, G.M. In *Crystallographic Computing 6*; Flack, H. D., Parkanyi, L., Simon, K., Eds.; Oxford University Press: Oxford, 1993.

63.Flack, H.D. *Acta Crystallogr.* **1983**, *A39*, 876.

Bibliography

Albert, H.J. In *McGraw-Hill Encyclopedia of Science and Technology*, 6th Ed., S.P. Parker, Ed. Volume 12; McGraw-Hill: New York, 1987.

Berti, G.;Macchia, B.;Macchia,F. *Tetrahedron Letters* **1965**, *38*, 3421-3427.

Carey, F.A.; Sundberg, R.J. *Advanced Organic Chemistry*, 3rd Ed., Part A; Plenum: New York, 1990.

Coe, B.J. *Polyhedron* **1992**, *11*, no. 9, 1085-1091.

Corey, E.J.;Noe, M.C.; Sharsan, S. *J. Am. Chem. Soc.* **1993**,*115*, 3828-3829.

Criegee, R. *Justus Liebigs Ann. Chem.* **1936**, *522*, 75-96.

DelMonte, A.J.; Haller, J.; Houk, K.N.; Sharpless, K.B.; Singleton, D.A.; Strassner, T.; Thomas, A.A. *J. Am. Chem. Soc.* **1997**, *119*, 9907-9908.

Denmark, S.E.;Barsanti, P.A.;Wong, K.-T.;Stavanger, R.A. *J. Organic Chem.*, **1998**, *63*, 2428-2429.

Dunitz, J.D. *X-ray Analysis and the Structure of Organic Molecules*, 2nd Ed. Corrected Reprint; VCH publishers, Inc.: New York, 1995.

Enemarck, J.H.;Backes-Dahmann, G. *Inorganic Chem.* **1987**, *26*, 3960-3962.

Flack, H.D. *Acta Crystallogr.* **1983**, *A39*, 876.

Frenking, G.;Deubel, D.V. *J. Am. Chem. Soc.* **1999**, *121*, 2021-2031.

Gable, K.P. *Adv. Organomet. Chem.* **1997**, vol. 41, 127-161.

Gable, K.P. *Organometallics* **1994**, *13*, 2486-2488.

Gable, K.P.;AbuBaker, A.;Zientara, K.;Wainwright, A.M. *Organometallics* **1999**, *18*, 173-179.

Gable, K.P.;Juliette, J.J.J. *J. Am. Chem. Soc.* **1995**, *117*, 955-962.

Gable, K.P.;Juliette, J.J.J. *J. Am. Chem. Soc.* **1996**, *118*, 2625-2633.

Gable, K.P.; Phan, T.N. *J. Am. Chem. Soc.* **1993**, *115*, 3036-3037.

Gable, K.P.; Phan, T.N. *J. Am. Chem. Soc.* **1994**, *116*, 833-839.

Gobel, T.; Sharpless, K.B. *Angew. Chem. Int. Ed. Engl.* **1993**, *32*, no. 9,1329.

Herrmann, W.A. *Chem. Ber.* **1990**, *123*, 1347.

Herrmann, W.A.; Kuchler, J.G.; Weichselbaumer, G.; Herdtweck, E.; Kiprof, P.J. *Organomet. Chem.* **1989**, *372*, 351-370.

Herrmann, W.A.; Kuhn, F.E.; Rauch, M.U.; Correia, J.D.G.; Artus, G. *Inorg. Chem.* **1995**, *34*, 2914-2920.

Herrmann, W. A.; Marz, D.W.; Herdtwick, E.; Schafer, A.; Wagner, W.; Kneuper, H.-J. *Angew. Chem. Int. Ed. Engl.* **1987**, *26*, 462-464.

Hoeldrich, W.F. In *Heterogeneous Catalysis and Fine Chemicals*; M. Guisnet, Ed. Elsevier Science Publishers: Amsterdam, 1988.

Ittel, S.D.; Parshall, G.W. *Homogeneous Catalysis*, 2nd Ed.; John Wiley & Sons: New York, 1992.

Mayer, J.; Brown, S. *Inorganic Chem.* **1992**, *32*, 4091-4100.

Norrby, P.-O.; Gable, K.P. *J. Chem. Soc., Perkin Trans. 2* **1995**,171-178.

Norrby, P.-O.; Kolb, H.C.; Sharpless, K.B.; *Organometallics* **1994**, *13*, 344.

Nugent, W.A.;Mayer, J.M. *Metal-Ligand Multiple Bonds*, John Wiley & Sons: New York, 1988.

Palucki, M.; McCormick, G.J.; Jacobsen, E.N. *Tetrahedron Letters* **1995**, *36*, 5457-5460.

Paulo, A.; Domingos, A.; Marcalo, J.; Pires de Matos, A.; Santos, I. *Inorg. Chem.* **1995**, *34*, 2113-2120.

Periana, R.A.; Taube, D.J. *Science* **1993**, *259*, 340-343.

Periana, R.A.;Taube, D.J. *Science* **1998**, *280*, 560-564.

Sharpless, K.B. *J. Am. Chem. Soc.* **1977**, 3120.

Sheldrick, G.M. *Acta Crystallogr.* **1990**, *A46*, 467.

Sheldrick, G.M. In *Crystallographic Computing 6*; Flack, H.D.; Parkanyi, L.; Simon, K.; Eds.; Oxford University Press: Oxford, 1993.

Sheffield ChemPuter online, www.shef.ac.uk/~chem/chemputer/isotopes.html.

Shilov, A.E.; Shul'pin, G.B. *Chem. Rev.* **1997**, *97*, 2679-2932.

Shriver, D.F.; Drezdzon, M.A. *Manipulation of Air-Sensitive Compounds.* Wiley: New York, 1986.

Torrent, M.; Deng, L.; Duran, M.; Sola, M.; Ziegler, T. *Organometallics* **1997**, *16*, 13-19.

Veldkamp, A.; Frenking, G. *J. Am. Chem. Soc.* **1994**, *116*, 4937.

Williams, D.H.;Fleming, I. *Spectroscopic Methods in Organic Chemistry*, 5th Ed.; McGraw-Hill: London, 1995.

Yokochi, Alex–Chemistry Department, Oregon State University, e-mail address: alexy@crystal.chem.orst.edu

APPENDIX

Appendix. Crystallographic Data

Table A.1: Crystal Data and Structure Refinement for $[Re(N_2C_3H_2Me_2)_2(Cl)_2O]_2$-$\mu_2$-O•$CHCl_3$

Indentification code	Str 15
Empirical Formula	$C_{21}H_{29}Cl_7N_8O_3Re_2$
Formula Weight	1062.07
Temperature	298(2) K
Wavelength	1.54178 Å
Crystal system	Monoclinic
Space group	$P2_1$
Unit cell dimensions	a = 9.9936(6) Å α = 90°
	b = 15.9596(11) Å β = 96.892(4)°
	c = 11.1895(5) Å γ = 90°
Volume	1771.76(18) $Å^3$
Z	2
Density (calculated)	1.991 Mg/m^3
Absorption coefficient	18.319 mm^{-1}
F(000)	1008
Crystal size	0.30 X 0.30 X 0.10 mm^3
Theta range for data collection	3.98 to 57.19°
Index ranges	-2<=h<=10,-17<=k<=5,-12<=l<=11
Reflections collected	3182
Independent reflections	2666 [R(int) = 0.1062]
Absorption correction	Analytical (face indexing)
Max. and min. transmission	0.2617 and 0.0729
Refinement method	Full-matrix least-squares on F^2
Data / restraints / parameters	2666 / 1 / 382
Goodness-of-fit on F^2	1.118
Final R indices [I>2sigma(I)]	R1 = 0.0518, wR2 = 0.1169
R indices (all data)	R1 = 0.0526, wR2 = 0.1187
Absolute structure parameter	0.43(5)
Extinction coefficient	0.0018(2)
Largest diff. peak and hole	1.436 and -0.679 e.$Å^{-3}$

Table A.2: Atomic Coordinates (X 10^4) and Equivalent Isotropic Displacement Parameters ($Å^2$ X 10^3) for $[Re(N_2C_3H_2Me_2)_2(Cl)_2O]_2$-$\mu_2$-O•$CHCl_3$

(U(eq) is defined as one third of the trace of the orthogonalized Uij tensor.)

	x	y	z	U(eq)
Re(1)	2169(1)	3007(1)	9216(1)	82(1)
Re(2)	2263(1)	1987(1)	6103(1)	82(1)
Cl(11)	-200(4)	3222(3)	8653(4)	94(1)
Cl(12)	2641(5)	4334(3)	8336(5)	98(1)
Cl(21)	-63(4)	1617(3)	6167(4)	93(1)
Cl(22)	3011(5)	718(3)	7131(4)	100(1)
O(1)	2242(11)	2522(9)	7658(14)	94(3)
O(2)	2183(14)	3346(12)	10610(16)	114(4)
O(3)	2281(13)	1673(11)	4730(13)	103(4)
N(11)	1772(14)	1788(12)	9753(13)	97(4)
N(12)	796(15)	1341(11)	9023(15)	97(4)
C(13)	720(2)	543(11)	9452(18)	97(5)
C(14)	1590(2)	502(13)	10519(18)	105(6)
C(15)	2260(2)	1270(15)	10662(18)	101(6)
C(16)	3300(3)	1539(18)	11600(2)	129(7)
C(17)	-150(2)	-89(15)	8770(2)	120(7)
N(21)	4248(14)	2772(11)	9502(11)	91(4)
N(22)	4743(14)	2035(11)	9090(14)	96(4)
C(23)	6095(17)	2000(18)	9324(19)	107(5)
C(24)	6465(17)	2719(18)	9961(18)	112(7)
C(25)	5320(18)	3193(17)	10023(17)	106(6)
C(26)	5230(2)	4000(2)	10680(3)	137(8)
C(27)	6880(3)	1285(19)	8970(3)	135(9)
N(31)	4238(13)	2412(11)	6253(12)	84(4)
N(32)	4528(14)	3183(11)	6723(13)	92(4)
C(33)	5830(2)	3388(19)	6710(2)	122(8)
C(34)	6450(2)	2720(2)	6250(2)	124(8)
C(35)	5445(18)	2129(17)	5960(2)	110(6)
C(36)	5460(3)	1303(16)	5280(3)	133(9)
C(37)	6370(2)	4200(2)	7220(3)	142(10)
N(41)	1643(14)	3177(13)	5463(12)	99(5)
N(42)	632(14)	3608(10)	5913(13)	90(5)
C(43)	447(17)	4373(12)	5488(18)	93(5)
C(44)	1350(2)	4482(12)	4676(19)	102(5)

C(45)	2060(2)	3742(15)	4630(2)	101(5)
C(46)	3170(3)	3522(18)	3900(2)	118(7)
C(47)	-580(3)	4930(2)	5940(3)	137(9)
C(1)	-1200(3)	2430(3)	3150(2)	146(11)
Cl(1)	-2258(15)	1506(9)	2785(10)	212(5)
Cl(2)	-2125(13)	3264(10)	3319(9)	206(5)
Cl(3)	-127(7)	2524(8)	2088(8)	163(3)

Table A.3: Selected Bond Lengths [Å] and Angles [°] for $[Re(N_2C_3H_2Me_2)_2(Cl)_2O]_2$-$\mu_2$-O•$CHCl_3$

Re(1)-O(2)	1.649(18)
Re(1)-O(1)	1.917(15)
Re(1)-N(11)	2.089(18)
Re(1)-N(21)	2.097(14)
Re(1)-Cl(11)	2.401(4)
Re(1)-Cl(12)	2.405(5)
Re(2)-O(3)	1.618(14)
Re(2)-O(1)	1.942(15)
Re(2)-N(31)	2.074(14)
Re(2)-N(41)	2.10(2)
Re(2)-Cl(22)	2.403(5)
Re(2)-Cl(21)	2.408(4)

O(2)-Re(1)-O(1)	174.6(8)
O(2)-Re(1)-N(11)	90.7(8)
O(1)-Re(1)-N(11)	85.1(6)
O(2)-Re(1)-N(21)	91.1(6)
O(1)-Re(1)-N(21)	85.5(5)
N(11)-Re(1)-N(21)	90.5(6)
O(2)-Re(1)-Cl(11)	95.6(5)
O(1)-Re(1)-Cl(11)	87.9(3)
N(11)-Re(1)-Cl(11)	89.6(4)
N(21)-Re(1)-Cl(11)	173.3(4)
O(2)-Re(1)-Cl(12)	96.8(7)
O(1)-Re(1)-Cl(12)	87.3(5)
N(11)-Re(1)-Cl(12)	172.4(4)
N(21)-Re(1)-Cl(12)	88.9(5)
Cl(11)-Re(1)-Cl(12)	90.15(16)
O(3)-Re(2)-O(1)	171.9(8)
O(3)-Re(2)-N(31)	93.4(6)
O(1)-Re(2)-N(31)	84.0(5)

O(3)-Re(2)-N(41)	89.6(7)
O(1)-Re(2)-N(41)	82.7(6)
N(31)-Re(2)-N(41)	88.3(6)
O(3)-Re(2)-Cl(22)	98.9(6)
O(1)-Re(2)-Cl(22)	88.7(4)
N(31)-Re(2)-Cl(22)	89.9(5)
N(41)-Re(2)-Cl(22)	171.4(4)
O(3)-Re(2)-Cl(21)	94.2(5)
O(1)-Re(2)-Cl(21)	88.1(4)
N(31)-Re(2)-Cl(21)	172.0(4)
N(41)-Re(2)-Cl(21)	89.2(4)
Cl(22)-Re(2)-Cl(21)	91.42(17)
Re(1)-O(1)-Re(2)	177.2(9)

Table A.4: Bond Lengths [Å] and Angles [°] for $[Re(N_2C_3H_2Me_2)_2(Cl)_2O]_2$-$\mu_2$-O•$CHCl_3$

Re(1)-O(2)	1.649(18)
Re(1)-O(1)	1.917(15)
Re(1)-N(11)	2.089(18)
Re(1)-N(21)	2.097(14)
Re(1)-Cl(11)	2.401(4)
Re(1)-Cl(12)	2.405(5)
Re(2)-O(3)	1.618(14)
Re(2)-O(1)	1.942(15)
Re(2)-N(31)	2.074(14)
Re(2)-N(41)	2.10(2)
Re(2)-Cl(22)	2.403(5)
Re(2)-Cl(21)	2.408(4)
N(11)-C(15)	1.36(3)
N(11)-N(12)	1.39(2)
N(12)-C(13)	1.37(2)
C(13)-C(14)	1.39(3)
C(13)-C(17)	1.48(3)
C(14)-C(15)	1.40(3)
C(15)-C(16)	1.46(3)
N(21)-C(25)	1.34(3)
N(21)-N(22)	1.38(2)
N(22)-C(23)	1.35(2)
C(23)-C(24)	1.38(4)
C(23)-C(27)	1.47(3)

C(24)-C(25)	1.38(3)
C(25)-C(26)	1.49(4)
N(31)-N(32)	1.36(2)
N(31)-C(35)	1.37(2)
N(32)-C(33)	1.35(3)
C(33)-C(34)	1.36(4)
C(33)-C(37)	1.50(4)
C(34)-C(35)	1.39(3)
C(35)-C(36)	1.52(3)
N(41)-N(42)	1.37(2)
N(41)-C(45)	1.40(3)
N(42)-C(43)	1.32(2)
C(43)-C(44)	1.36(3)
C(43)-C(47)	1.49(3)
C(44)-C(45)	1.39(3)
C(45)-C(46)	1.49(3)
C(1)-Cl(2)	1.64(4)
C(1)-Cl(3)	1.70(3)
C(1)-Cl(1)	1.83(4)

O(2)-Re(1)-O(1)	174.6(8)
O(2)-Re(1)-N(11)	90.7(8)
O(1)-Re(1)-N(11)	85.1(6)
O(2)-Re(1)-N(21)	91.1(6)
O(1)-Re(1)-N(21)	85.5(5)
N(11)-Re(1)-N(21)	90.5(6)
O(2)-Re(1)-Cl(11)	95.6(5)
O(1)-Re(1)-Cl(11)	87.9(3)
N(11)-Re(1)-Cl(11)	89.6(4)
N(21)-Re(1)-Cl(11)	173.3(4)
O(2)-Re(1)-Cl(12)	96.8(7)
O(1)-Re(1)-Cl(12)	87.3(5)
N(11)-Re(1)-Cl(12)	172.4(4)
N(21)-Re(1)-Cl(12)	88.9(5)
Cl(11)-Re(1)-Cl(12)	90.15(16)
O(3)-Re(2)-O(1)	171.9(8)
O(3)-Re(2)-N(31)	93.4(6)
O(1)-Re(2)-N(31)	84.0(5)
O(3)-Re(2)-N(41)	89.6(7)
O(1)-Re(2)-N(41)	82.7(6)
N(31)-Re(2)-N(41)	88.3(6)
O(3)-Re(2)-Cl(22)	98.9(6)
O(1)-Re(2)-Cl(22)	88.7(4)
N(31)-Re(2)-Cl(22)	89.9(5)

N(41)-Re(2)-Cl(22)	171.4(4)
O(3)-Re(2)-Cl(21)	94.2(5)
O(1)-Re(2)-Cl(21)	88.1(4)
N(31)-Re(2)-Cl(21)	172.0(4)
N(41)-Re(2)-Cl(21)	89.2(4)
Cl(22)-Re(2)-Cl(21)	91.42(17)
Re(1)-O(1)-Re(2)	177.2(9)
C(15)-N(11)-N(12)	106.9(18)
C(15)-N(11)-Re(1)	136.1(16)
N(12)-N(11)-Re(1)	116.9(11)
C(13)-N(12)-N(11)	109.6(16)
N(12)-C(13)-C(14)	106.9(18)
N(12)-C(13)-C(17)	120.4(19)
C(14)-C(13)-C(17)	132.6(18)
C(13)-C(14)-C(15)	107.3(18)
N(11)-C(15)-C(14)	109(2)
N(11)-C(15)-C(16)	122(2)
C(14)-C(15)-C(16)	129(2)
C(25)-N(21)-N(22)	105.9(15)
C(25)-N(21)-Re(1)	134.7(15)
N(22)-N(21)-Re(1)	119.4(11)
C(23)-N(22)-N(21)	111.3(18)
N(22)-C(23)-C(24)	105.4(18)
N(22)-C(23)-C(27)	123(2)
C(24)-C(23)-C(27)	132.0(19)
C(23)-C(24)-C(25)	108.0(17)
N(21)-C(25)-C(24)	109(2)
N(21)-C(25)-C(26)	123.7(18)
C(24)-C(25)-C(26)	127(2)
N(32)-N(31)-C(35)	103.9(16)
N(32)-N(31)-Re(2)	119.1(10)
C(35)-N(31)-Re(2)	137.0(15)
C(33)-N(32)-N(31)	112.2(18)
N(32)-C(33)-C(34)	107(2)
N(32)-C(33)-C(37)	121(2)
C(34)-C(33)-C(37)	132(2)
C(33)-C(34)-C(35)	105.9(19)
N(31)-C(35)-C(34)	111(2)
N(31)-C(35)-C(36)	118.0(19)
C(34)-C(35)-C(36)	131(2)
N(42)-N(41)-C(45)	102.5(18)
N(42)-N(41)-Re(2)	122.1(11)
C(45)-N(41)-Re(2)	135.4(15)
C(43)-N(42)-N(41)	114.3(15)

N(42)-C(43)-C(44)	106.5(16)
N(42)-C(43)-C(47)	120.2(17)
C(44)-C(43)-C(47)	133.3(18)
C(43)-C(44)-C(45)	107.5(18)
C(44)-C(45)-N(41)	109(2)
C(44)-C(45)-C(46)	130(2)
N(41)-C(45)-C(46)	121(2)
Cl(2)-C(1)-Cl(3)	115(2)
Cl(2)-C(1)-Cl(1)	111.3(16)
Cl(3)-C(1)-Cl(1)	108(2)

Table A.5: Anisotropic Displacement Parameters (Å X 10^3) for $[Re(N_2C_3H_2Me_2)_2(Cl)_2O]_2$-$\mu_2$-O•$CHCl_3$

The anisotropic displacement factor exponent takes the form:
$-2\pi^2[h^2a^{*2}U11 + ... + 2\ h\ k\ a^*\ b^*\ U12]$

	U11	U22	U33	U23	U13	U12
Re(1)	81(1)	87(1)	79(1)	-3(1)	12(1)	5(1)
Re(2)	83(1)	85(1)	79(1)	-3(1)	12(1)	-3(1)
Cl(11)	83(2)	106(3)	95(2)	6(2)	17(2)	11(2)
Cl(12)	102(2)	84(2)	107(3)	2(2)	7(2)	-1(2)
Cl(21)	85(2)	95(2)	97(2)	4(2)	5(2)	-14(2)
Cl(22)	107(2)	88(2)	107(3)	4(2)	18(2)	14(2)
O(1)	72(5)	80(6)	126(9)	-8(6)	2(5)	3(5)
O(2)	95(8)	130(12)	118(10)	-7(9)	10(6)	11(7)
O(3)	93(7)	122(10)	94(8)	-8(8)	14(5)	-13(7)
N(11)	87(7)	119(12)	88(8)	6(8)	15(6)	12(8)
N(12)	86(8)	102(10)	105(10)	5(8)	22(7)	7(7)
C(13)	117(12)	72(9)	108(13)	20(9)	41(10)	-1(8)
C(14)	143(16)	82(10)	88(12)	26(9)	13(11)	3(11)
C(15)	117(13)	115(15)	76(11)	10(11)	30(9)	29(12)
C(16)	160(19)	122(17)	102(14)	17(14)	5(13)	11(16)
C(17)	123(14)	98(13)	143(19)	22(13)	28(12)	-24(12)
N(21)	99(9)	111(11)	63(6)	12(7)	8(6)	-14(8)
N(22)	91(8)	87(8)	109(10)	-7(9)	8(7)	10(8)
C(23)	80(9)	128(14)	111(12)	-16(14)	5(8)	23(12)
C(24)	75(9)	160(2)	94(11)	2(13)	0(8)	-11(11)

C(25)	92(11)	140(18)	85(10)	0(11)	10(8)	6(11)
C(26)	109(13)	142(19)	150(2)	-18(19)	-15(13)	-16(15)
C(27)	110(13)	134(19)	160(2)	-18(17)	21(13)	52(14)
N(31)	88(7)	97(8)	72(7)	-19(7)	23(6)	18(7)
N(32)	84(7)	111(11)	87(8)	5(8)	30(6)	0(7)
C(33)	85(11)	160(2)	115(15)	-8(16)	8(10)	-14(13)
C(34)	92(12)	160(2)	128(17)	-15(16)	38(11)	-14(13)
C(35)	82(9)	130(17)	115(13)	-2(13)	4(9)	8(11)
C(36)	139(17)	110(15)	160(2)	-16(15)	57(16)	42(14)
C(37)	96(12)	150(2)	170(2)	-40(2)	11(13)	-27(15)
N(41)	92(8)	138(14)	69(7)	12(8)	10(6)	-11(9)
N(42)	93(8)	98(10)	81(9)	8(8)	21(6)	-4(7)
C(43)	86(9)	95(11)	101(12)	29(9)	25(8)	19(8)
C(44)	125(14)	80(10)	99(12)	17(9)	7(10)	11(10)
C(45)	94(10)	107(14)	103(13)	15(12)	9(9)	-20(10)
C(46)	132(15)	118(16)	110(14)	26(13)	33(11)	-6(13)
C(47)	125(15)	140(2)	150(2)	38(18)	44(14)	33(16)
C(1)	136(17)	210(3)	91(13)	45(17)	8(12)	0(19)
Cl(1)	234(10)	219(10)	175(8)	48(8)	-13(7)	-98(9)
Cl(2)	206(9)	266(15)	144(6)	-22(8)	9(5)	71(9)
Cl(3)	128(4)	203(8)	160(6)	27(6)	24(4)	9(5)

Table A.6: Hydrogen Coordinates (X 10^4) and Isotropic Displacement Parameters ($Å^2$ X 10^3) for $[Re(N_2C_3H_2Me_2)_2(Cl)_2O]_2$-$\mu_2$-O•$CHCl_3$

	x	y	z	U(eq)
H(12)	60(10)	1640(4)	8070(13)	90(3)
H(14)	1660(3)	190(10)	10880(11)	69(19)
H(16A)	3949	1880	11257	194
H(16B)	3750	1056	11977	194
H(16C)	2905	1857	12196	194
H(17A)	378	-402	8258	180
H(17B)	-872	188	8286	180
H(17C)	-506	-464	9322	180
H(22)	4330(12)	1710(9)	8790(9)	90(3)
H(24)	7370(14)	2870(3)	10310(5)	69(19)
H(26A)	4943	4435	10111	206
H(26B)	6095	4138	11095	206
H(26C)	4586	3945	11245	206

H(27A)	6388	776	9045	203
H(27B)	7726	1258	9477	203
H(27C)	7050	1353	8145	203
H(32)	4040(14)	3450(8)	6960(7)	90(3)
H(34)	7380(15)	2670(2)	6150(3)	69(19)
H(36A)	4985	886	5684	199
H(36B)	6378	1126	5266	199
H(36C)	5036	1375	4475	199
H(37A)	6526	4576	6575	213
H(37B)	7204	4110	7724	213
H(37C)	5729	4452	7686	213
H(42)	400(14)	3500(6)	6170(15)	90(3)
H(44)	1470(3)	5000(9)	4200(8)	69(19)
H(46A)	3979	3814	4217	178
H(46B)	2919	3682	3082	178
H(46C)	3330	2929	3948	178
H(47A)	-1468	4721	5665	205
H(47B)	-491	5487	5634	205
H(47C)	-453	4940	6801	205
H(1)	-658	2327	3921	175

Table A.7: Torsion Angles [°] for $[Re(N_2C_3H_2Me_2)_2(Cl)_2O]_2$-$\mu_2$-O•$CHCl_3$

O(2)-Re(1)-O(1)-Re(2)	64(17)
N(11)-Re(1)-O(1)-Re(2)	23(15)
N(21)-Re(1)-O(1)-Re(2)	114(15)
Cl(11)-Re(1)-O(1)-Re(2)	-66(15)
Cl(12)-Re(1)-O(1)-Re(2)	-157(15)
O(3)-Re(2)-O(1)-Re(1)	146(13)
N(31)-Re(2)-O(1)-Re(1)	-143(15)
N(41)-Re(2)-O(1)-Re(1)	128(15)
Cl(22)-Re(2)-O(1)-Re(1)	-53(15)
Cl(21)-Re(2)-O(1)-Re(1)	39(15)
O(2)-Re(1)-N(11)-C(15)	-46.1(18)
O(1)-Re(1)-N(11)-C(15)	130.4(17)
N(21)-Re(1)-N(11)-C(15)	45.0(17)
Cl(11)-Re(1)-N(11)-C(15)	-141.7(17)
Cl(12)-Re(1)-N(11)-C(15)	130(3)
O(2)-Re(1)-N(11)-N(12)	136.2(12)
O(1)-Re(1)-N(11)-N(12)	-47.3(11)
N(21)-Re(1)-N(11)-N(12)	-132.7(12)

Cl(11)-Re(1)-N(11)-N(12)	40.6(11)
Cl(12)-Re(1)-N(11)-N(12)	-47(4)
C(15)-N(11)-N(12)-C(13)	-2.4(19)
Re(1)-N(11)-N(12)-C(13)	175.9(11)
N(11)-N(12)-C(13)-C(14)	5(2)
N(11)-N(12)-C(13)-C(17)	-174.0(17)
N(12)-C(13)-C(14)-C(15)	-5(2)
C(17)-C(13)-C(14)-C(15)	173(2)
N(12)-N(11)-C(15)-C(14)	-1(2)
Re(1)-N(11)-C(15)-C(14)	-178.6(13)
N(12)-N(11)-C(15)-C(16)	-179.9(19)
Re(1)-N(11)-C(15)-C(16)	2(3)
C(13)-C(14)-C(15)-N(11)	3(2)
C(13)-C(14)-C(15)-C(16)	-177(2)
O(2)-Re(1)-N(21)-C(25)	-44.7(18)
O(1)-Re(1)-N(21)-C(25)	139.5(17)
N(11)-Re(1)-N(21)-C(25)	-135.5(17)
Cl(11)-Re(1)-N(21)-C(25)	134(4)
Cl(12)-Re(1)-N(21)-C(25)	52.1(17)
O(2)-Re(1)-N(21)-N(22)	135.9(13)
O(1)-Re(1)-N(21)-N(22)	-39.9(12)
N(11)-Re(1)-N(21)-N(22)	45.1(11)
Cl(11)-Re(1)-N(21)-N(22)	-45(5)
Cl(12)-Re(1)-N(21)-N(22)	-127.3(11)
C(25)-N(21)-N(22)-C(23)	-1(2)
Re(1)-N(21)-N(22)-C(23)	178.4(14)
N(21)-N(22)-C(23)-C(24)	3(2)
N(21)-N(22)-C(23)-C(27)	-179(2)
N(22)-C(23)-C(24)-C(25)	-4(3)
C(27)-C(23)-C(24)-C(25)	179(3)
N(22)-N(21)-C(25)-C(24)	-1(2)
Re(1)-N(21)-C(25)-C(24)	179.2(13)
N(22)-N(21)-C(25)-C(26)	-175(2)
Re(1)-N(21)-C(25)-C(26)	6(3)
C(23)-C(24)-C(25)-N(21)	3(3)
C(23)-C(24)-C(25)-C(26)	177(2)
O(3)-Re(2)-N(31)-N(32)	132.9(13)
O(1)-Re(2)-N(31)-N(32)	-39.4(12)
N(41)-Re(2)-N(31)-N(32)	43.4(12)
Cl(22)-Re(2)-N(31)-N(32)	-128.1(12)
Cl(21)-Re(2)-N(31)-N(32)	-28(4)
O(3)-Re(2)-N(31)-C(35)	-44(2)
O(1)-Re(2)-N(31)-C(35)	143(2)
N(41)-Re(2)-N(31)-C(35)	-133.8(19)

Cl(22)-Re(2)-N(31)-C(35)	54.6(19)
Cl(21)-Re(2)-N(31)-C(35)	154(3)
C(35)-N(31)-N(32)-C(33)	1(2)
Re(2)-N(31)-N(32)-C(33)	-176.9(15)
N(31)-N(32)-C(33)-C(34)	-2(3)
N(31)-N(32)-C(33)-C(37)	-178(2)
N(32)-C(33)-C(34)-C(35)	2(3)
C(37)-C(33)-C(34)-C(35)	178(3)
N(32)-N(31)-C(35)-C(34)	0(2)
Re(2)-N(31)-C(35)-C(34)	177.9(16)
N(32)-N(31)-C(35)-C(36)	-174.0(19)
Re(2)-N(31)-C(35)-C(36)	3(3)
C(33)-C(34)-C(35)-N(31)	-2(3)
C(33)-C(34)-C(35)-C(36)	172(2)
O(3)-Re(2)-N(41)-N(42)	135.3(13)
O(1)-Re(2)-N(41)-N(42)	-47.1(13)
N(31)-Re(2)-N(41)-N(42)	-131.3(13)
Cl(22)-Re(2)-N(41)-N(42)	-53(3)
Cl(21)-Re(2)-N(41)-N(42)	41.1(13)
O(3)-Re(2)-N(41)-C(45)	-48.5(19)
O(1)-Re(2)-N(41)-C(45)	129.1(19)
N(31)-Re(2)-N(41)-C(45)	45.0(18)
Cl(22)-Re(2)-N(41)-C(45)	123(3)
Cl(21)-Re(2)-N(41)-C(45)	-142.7(18)
C(45)-N(41)-N(42)-C(43)	-3(2)
Re(2)-N(41)-N(42)-C(43)	174.4(13)
N(41)-N(42)-C(43)-C(44)	1(2)
N(41)-N(42)-C(43)-C(47)	-177(2)
N(42)-C(43)-C(44)-C(45)	1(2)
C(47)-C(43)-C(44)-C(45)	179(3)
C(43)-C(44)-C(45)-N(41)	-2(3)
C(43)-C(44)-C(45)-C(46)	-180(2)
N(42)-N(41)-C(45)-C(44)	3(2)
Re(2)-N(41)-C(45)-C(44)	-173.6(13)
N(42)-N(41)-C(45)-C(46)	-179.5(19)
Re(2)-N(41)-C(45)-C(46)	4(3)